UNIVERSITÉ DU QUÉBEC À MONTRÉAL

IMPACTS DU GEL PAR COLLISION SUR LA PRODUCTION DE PLUIE VERGLAÇANTE

MÉMOIRE

PRÉSENTÉ

COMME EXIGENCE PARTIELLE

DE LA MAÎTRISE EN SCIENCES DES LA TERRE ET DE L'ATMOSPHÈRE

PAR

AGNIESZKA BARSZCZ

MARS 2017

REMERCIEMENTS

Je tiens à remercier ma directrice de recherche Mme Julie Mireille Thériault et mon co-superviseur Jason Milbrandt pour leur patience, aide et précieux conseils.

Pour son soutien inconditionnel, je tiens à remercier mon mari Cédric. Sans lui, je n'aurais pas pu terminer ce travail. Je tiens aussi à remercier mon garçon Mathieu, qui m'a soutenue, et m'a fait rire de nombreuses fois lorsque j'en avais besoin.

Je voudrais aussi remercier MM. Donald Talbot, Lewis Poulin, Stéphane Gagnon et André Méthot pour m'avoir donné du temps et des ressources matérielles pour ce projet, de m'avoir soutenue et de nombreuses fois encouragée à le réaliser.

Finalement je tiens aussi à remercier Mme Anna Glazer qui m'a beaucoup aidée avec le coté informatique du projet.

Merci !

TABLE DES MATIÈRES

LISTE DES TABLEAUX

LISTE DES FIGURES

LISTE DES ABRÉVIATIONS, SIGLES, ET ACRONYMES

CMC Canadian Meteorological Center

ECCC Environnement et Changement climatique Canada

FZRA Freezing rain

GEM Global Environmental Multiscale

GS Graupel

HRDPS High Resolution Deterministic Prediction System

IP Ice pellets

ISBA Interactions between Soil, Biosphere, and Atmosphere surface scheme

LAM Limited area model

MY2 Milbrandt-Yau microphysics scheme

NWP Numerical weather prediction

RA Rain

SHRPD Système à Haute Résolution de Prévision Déterministe

SRPD Système Régional de Prévision Déterministe

UTC Coordinated Universal Time

RÉSUMÉ

La pluie verglaçante peut avoir des impacts importants sur la sécurité des réseaux routiers ainsi que sur les réseaux de transport électriques. Les processus conduisant à la formation de la pluie verglaçante sont complexes, car ce phénomène se produit lorsque la température de l'air avoisine 0°C. À ces températures, les types de précipitation observés peuvent être nombreux. Ces précipitations peuvent interagir entre elles pour en former de nouvelles, ainsi qu'en éliminer d'autres. Leur paramétrage peut rapidement devenir long en temps de calcul, et donc plusieurs hypothèses et simplifications doivent être faites lorsque des schémas microphysiques sont élaborés. Le but de cette étude est d'examiner l'impact du paramétrage du gel par collision sur les quantités de pluie verglaçante prévues en surface. Une tempête pour laquelle le Système à Haute Résolution de Prévision Déterministe (SHRPD) du Centre Météorologique Canadien (CMC) a sous prévu les quantités de pluie verglaçante a été identifiée. Le 24 décembre 2014, ce modèle prévoyait au plus 2 mm de verglas, alors que plus de 20 mm ont été observés à certains endroits dans le sud du Québec. Une étude de sensibilité a été menée sur un sous domaine du SHRPD couplé avec le schéma microphysique de Milbrandt and Yau (2005a). Tout d'abord, une température seuil pour le regel des gouttes de pluie causé par le gel par collision a été introduite. Ensuite, l'impact d'une variation systématique de l'efficacité de collecte entre les particules solides et liquides a été analysé. Il a été démontré que le terme de gel par collision entre les particules de pluie et de graupel est responsable de l'élimination de la pluie verglaçante dans ce schéma. Des températures seuil de regel plus froides, et des efficacités de

collectes plus basses favorisent la présence de pluie verglaçante en surface. Il a aussi été démontré que la présence d'une petite quantité de précipitations solides est suffisante pour causer le regel d'une grande quantité de pluie verglaçante. Pour conclure, la température à laquelle les gouttes d'eau regèlent en présence de glace est critique, car elle peut causer l'élimination de la pluie verglaçante en surface. Une représentation plus détaillée de ces processus en introduisant des particules semi-liquides dans le schéma microphysique serait donc souhaitable.

Mots-clés Pluie verglaçante, Grésil, Gel par collision, Collection

CHAPITRE I

INTRODUCTION

Plusieurs catastrophes naturelles relativement récentes ont été causées par des précipitations impliquant des changements de phases. On peut notamment penser aux inondations de Calgary en 2013 et à la crise du verglas en 1998 au Québec. Ces deux événements ont causé des milliards de dollars en dommages et ont eu un impact direct sur un grand nombre de personnes. La pluie verglaçante, qui est un phénomène hivernal impliquant un changement de phase, se produit lorsque des précipitations liquides, ayant une température inférieure à 0°C, gèlent instantanément au contact d'une surface glacée. Il se forme alors une couche de glace translucide que l'on appelle verglas. Au Québec, on observe de la pluie verglaçante en moyenne 50 h par année dans la vallée du Saint-Laurent (Cortinas *et al.*, 2004). Tous ces événements de pluie verglaçante ne sont pas aussi catastrophiques que la tempête de 1998 ; par contre les impacts de cette pluie verglaçante sur la société sont nombreux : routes et trottoirs glissants, pertes de contrôle des automobilistes, pannes de courant, etc. La sécurité des avions peut aussi en être affectée.

La prévision de la pluie verglaçante est très importante pour limiter les dégâts qu'elle peut causer en ayant une meilleure préparation avant son arrivée. Par exemple, les villes épandent du sel sur les routes pour éviter qu'elles ne

deviennent glissantes sous l'influence du verglas. Des avertissements publics peuvent être émis pour prévenir les gens et diminuer le nombre d'accidents sur les routes. Les compagnies qui gèrent les infrastructures électriques doivent aussi se préparer en vue de nombreuses pannes de courant. Finalement, les compagnies aériennes peuvent changer leurs plans de vol pour éviter des conditions dangereuses et choisir un liquide dégivrant approprié. Il est donc primordial de bien comprendre les processus de formation de la pluie verglaçante afin de bien les représenter dans les modèles numériques de prévisions du temps. Ceci permet d'anticiper sa formation, et de bien s'y préparer.

En avant des fronts chauds associés aux dépressions des latitudes moyennes, on observe parfois la formation d'une inversion de température. Celle-ci peut être formée d'une couche d'air chaud ($> 0°C$) en altitude et une couche d'air froid ($< 0°C$) près de la surface (Figure 2.1). Loin en avant du front chaud, lorsque la température de l'air reste inférieure à $0°C$, les précipitations glacées formées en altitude ne fondent pas. À la surface, on observe alors de la neige. Plus près du front chaud, les précipitations fondent graduellement dans la couche chaude. Si celle-ci est mince, alors les flocons fondent partiellement en la traversant et leur regel est initié par la glace restante dans la particule. Ce processus est la source principale de formation du grésil observé en surface (Hanesiak and Stewart, 1995; Zerr, 1997). Lorsque la couche d'air chaud est épaisse, toutes les particules glacées qui la traversent fondent entièrement. Ces gouttes d'eau sont surfondues lors de leur passage dans la couche d'air froid, et ne gèlent généralement qu'au contact avec une surface glacée. Ceci est le processus classique de formation de pluie verglaçante (Pruppacher and Klett, 1997).

Lorsque la température de l'air avoisine le point de congélation, plusieurs types de précipitations peuvent donc être observés : pluie, pluie verglaçante, grésil, neige mouillée, ou neige. Ceux-ci peuvent être observés en même temps, ou les

uns à la suite des autres (Stewart, 1992; Cortinas *et al.*, 2004). Ces précipitations peuvent interagir ensemble pour en créer des nouvelles, tout en en éliminant d'autres (Stewart *et al.*, 2015). Par exemple, le gel par collision peut modifier significativement les quantités de pluie verglaçante en surface (Stewart and Crawford, 1995; Zerr, 1997; Gibson and Stewart, 2007). Il est donc primordial de bien comprendre ce phénomène et les subtilités de son paramétrage dans les modèles numériques, pour cerner son impact sur les prévisions de pluie verglaçante.

Généralement, les hydrométéores qui sont complètement liquides lors de leur entrée dans la couche de regel, ne gèlent pas d'une façon spontannée. Pour geler, ceux-ci doivent soit contenir un noyeau glaçongène, ou être refroidi à une température inférieure à $-38°C$ (Rogers and Yau, 1989). En effet, ce n'est qu'à cette température que les mollécules d'eau peuvent s'aligner spontanément pour former une structure cristalline et initier le gel des gouttes (Bigg, 1953; Rogers and Yau, 1989; Pruppacher and Klett, 1997).

Il est généralement accepté que la nucléation de la glace dans une particule entièrement liquide peut survenir lorsque la température de l'air est inférieure à $-5°C$. À ces températures, des noyaux glaçogènes peuvent être actifs (Meyers *et al.*, 1992; Stewart and Crawford, 1995; Zerr, 1997). Cependant, la température d'activation des noyaux varie en fonction de leur composition, de leur taille et de l'humidité relative de l'environnement (Fletcher, 1958, 1969; Cooper, 1986; Meyers *et al.*, 1992). Le processus Hallett-Mossop (1974) peut aussi contribuer au gel des gouttes d'eau. Ce processus secondaire de formation de glace est actif lorsque la température de l'air se situe entre $-8°C$ et $-3°C$. Il consiste en des aiguilles de glace qui se forment lorsque la glace givre rapidement. Lorsqu'elles entrent en collision avec de l'eau surfondue, ces particules peuvent contribuer à la formation de grésil. Finalement, les gouttes

d'eau peuvent s'évaporer et cette vapeur peut ensuite se déposer sur une particule de glace (Pruppacher and Klett, 1997; Stewart *et al.*, 2015).

Lorsque la température de l'air est supérieure à $-5°C$, la nucléation de la glace dans une goutte entièrement liquide n'est généralement pas possible. Le gel de ces gouttes peut être initié par une collision avec une particule glacée. Plusieurs types de collisions entre les particules solides, liquides et en phase mixte sont possibles. Par exemple, une goutte d'eau surfondue peut entrer en contact avec une particule de glace, de neige, ou de grésil. Dans les deux premiers cas, la particule résultante sera une particule de grésil, dans le troisième ce sera plutôt un agrégat de grésil (Gibson and Stewart, 2007; Carmichael *et al.*, 2011).

Le gel par collision peut être un processus menant à une réduction significative des taux de précipitations verglaçantes en surface (Stewart and Crawford, 1995; Zerr, 1997; Gibson and Stewart, 2007; Carmichael *et al.*, 2011). Par exemple, dans une étude théorique, Carmichael *et al.* (2011) ont montré qu'avec une couche de regel d'une épaisseur de 1200 m et un taux de précipitation de 5 mm h^{-1}, la réduction du taux de précipitations verglaçantes pourrait être de 20%, pour les gouttes entièrement liquides ayant un diamètre maximal de 1 mm. Il a aussi été démontré que le taux de réduction de pluie verglaçante est proportionnel au taux de précipitation et à l'épaisseur de la couche de regel, et inversement proportionnel à la taille maximale des gouttes d'eau surfondue.

Les collisions entre les particules sont régies par une combinaison de forces gravitationnelles, électriques et aérodynamiques. Dans les nuages, la force de gravité est prédominante. Les particules qui tombent plus vite, appelées les collecteurs, entrent en collision avec les particules se trouvant sur leur trajectoire. Pourtant, seule une fraction de celles-ci entre réellement en contact avec le collecteur. Les autres particules sont éjectées de la trajectoire,

puisqu'elles suivent les lignes de courant qui se créent autour du collecteur. Cette fraction dépend de plusieurs facteurs : le ratio de taille des particules, leurs vitesses, leurs formes, leurs poids. Lorsqu'une collision survient, les particules peuvent s'agglomérer ou rebondir, pour ensuite se séparer. Le produit des fractions de collision et de coalescence est défini comme l'efficacité de collecte (Pitter and Pruppacher, 1974; Rogers and Yau, 1989; Cober and List, 1993; Khain *et al.*, 2001).

Lorsque le gel d'une goutte a été initié, celui-ci se produit en trois étapes. Premièrement, la surfusion de l'eau conduit à la croissance rapide du cristal de glace. Ce faisant, de la chaleur latente est libérée et ce processus continue jusqu'à ce que la température de la particule atteigne 0°C. La fraction de la goutte qui gèle durant la première phase est égale à $80/\Delta T$ où ΔT représente le degré de surfusion de la goutte en degrés Celcius (Pruppacher and Klett, 1997). Il y a généralement été observé que le gel se produit de l'extérieur vers l'intérieur de la particule. Il se forme alors une coquille autour de la goutte liquide (Hindmarsh *et al.*, 2003; Gibson and Stewart, 2007). Deuxièmement, le gel continue du à un échange d'énergie entre la particule et son environnement. Durant cette étape, la température de la particule reste stable à 0°C. Cette étape est plus longue que la première (Pruppacher and Klett, 1997; Hindmarsh *et al.*, 2003). Il a d'ailleurs été démontré que la majorité des hydrométéores sous une inversion chaude n'est pas complètement gelée avant d'arriver au sol. Par exemple, il a été démontré dans une étude théorique qu'avec une température de l'environnement inférieure à -2°C et une couche de regel d'une hauteur 1000 m, seule les particules dont le diamètre est inférieur à 2.5 mm seront entièrement gelées en arrivant au sol (Carmichael *et al.*, 2011). Troisièmement, lorsqu'une particule devient complètement glacée, sa température chute jusqu'à ce qu'elle soit égale à celle de l'environnement (Pruppacher and Klett, 1997; Hindmarsh *et al.*, 2003).

Tous ces processus de gel, tout comme la formation et l'évolution des nuages et de la précipitation sont typiquement représentées à l'aide de schémas microphysiques détaillés couplés à des modèles atmosphériques de prévision numérique. Il existe plusieurs types de schémas microphysiques dont les schémas de type bin (ex : Geresdi (1998)) et les schémas de type bulk (ex : Ferrier (1994); Thompson *et al.* (2004); Milbrandt and Yau (2005a,b); Hong and Lim (2006)). Les schémas de type bulk sont très fréquemment utilisés dans la communauté scientifique en raison de leur moindre coût de calcul. Dans les schémas bulk, la distribution en taille des hydrométéores est représentée par une fonction analytique (ex : Ferrier (1994); Thompson *et al.* (2004); Hong and Lim (2006); Milbrandt and Yau (2005a,b). Pour chaque type d'hydrométéores, 1, 2 ou 3 moments peuvent être prédits. Par exemple, dans un schéma à deux moments, la concentration totale et le rapport de mélange de chaque catégorie de particules sont généralement prédits. Ces deux quantités correspondent au $0^{\text{ième}}$ et $3^{\text{ième}}$ moment de la distribution analytique de taille des particules. Celle-ci est une fonction exponentielle inverse :

$$N(D) = N_0 exp(\lambda D) \tag{1.1}$$

où D représente le diamètre des particules, N leurs nombre, N_0 l'interception et λ le paramètre de pente.

Tous ces schémas microphysiques contiennent un paramétrage des collisions entre les particules solides et liquides. La majorité des schémas utilise l'équation de Verlinde *et al.* (1990) pour représenter ces collisions (ex : Ferrier (1994); Reisner *et al.* (1998); Cohard and Pinty (2000); Milbrandt and Yau (2005a,b); Straka and Mansell (2005); Saleeby and Cotton (2008)). Celle-ci suppose que toutes les collisions sont indépendantes les unes des autres. Le nombre de particules qui entrent en collision dépend de la concentration par volume du nombre de particules de chaque catégorie, de leur vitesse de chute, du diamètre et de l'efficacité de collecte. Le paramétrage de ces variables, ainsi que la façon de déterminer le type

de particules résultantes d'une collision varie selon les schémas. Par exemple, dans le schéma de Milbrandt and Yau (2005a), la classe des particules résultantes est déterminée selon la densité d'une particule créée lors de la collision. Cette densité est estimée selon la taille moyenne des particules de chaque catégorie impliquée lors de la collision. Par exemple, si le diamètre moyen des flocons entrant en collision est grand et celui des gouttes est petit, toutes les particules résultantes seront des flocons de neige. Si par contre, le diamètre des flocons moyens est petit et celui des gouttes est grand, les particules résultantes seront plutôt de la neige roulée, ou de la grêle. Dans le schéma de Reisner *et al.* (1998), lorsque des particules liquides et solides entrent en collision, une fraction de la masse de l'eau est transférée vers la particule solide et le reste est transféré vers la catégorie de la neige roulée. Finalement, dans d'autres schémas, les particules en phase mixte sont explicitement représentées. Dans ces schémas, lors des collisions entre des particules solides et liquides, celles-ci deviennent semi-liquides (ex : Ferrier (1994); Saleeby and Cotton (2008)).

La représentation de l'efficacité de collecte varie aussi selon les paramétrages. Certains schémas utilisent une efficacité de collecte de 1 pour les collisions entre les particules liquides et solides (ex : Reisner *et al.* (1998); Milbrandt and Yau (2005a,b); Straka and Mansell (2005)). D'autres utilisent un paramétrage différent dépendamment si la particule glacée est sèche ou mouillée (Ferrier, 1994). Finalement, Thompson *et al.* (2008) ainsi que Saleeby and Cotton (2008) utilisent un paramétrage en fonction des diamètres du collecteur et de la particule collectée. Leurs suppositions sont basées sur les résultats provenant de schémas bins.

Les mécanismes de formation de la pluie verglaçante et les interactions de celle-ci avec les autres hydrométéores sont complexes. Elles sont donc difficiles à représenter adéquatement dans les modèles numériques. Étant donné les impacts

de la pluie verglaçante et l'importance de sa prévision, le but de cette étude est d'examiner l'impact du gel par collision sur les quantités de pluie verglaçante qui arrivent au sol. Pour ce faire, un schéma microphysique à deux moments couplé à un modèle de prévision numérique est utilisé. Une étude de cas où ce phénomène a eu un impact significatif est présentée. La sensibilité d'un modèle numérique au paramétrage du gel par collision est explorée en faisant varier systématiquement une température seuil de regel ainsi que le paramètre d'efficacité de collecte.

Ce mémoire est organisé comme suit : un article rédigé en anglais est présenté au chapitre II, et il sera suivi d'une conclusion générale au chapitre III. Cet article comprend 7 sections. La première est une introduction comprenant la revue de littérature et le contexte de l'étude. La deuxième contient une étude de cas pour une tempête où la collecte par collision a joué un rôle clé pour la prévision des quantités de pluie verglaçante. Dans la troisième section, les modèles utilisés ainsi que la méthodologie pour cette étude sont présentés. Dans la quatrième, les hydrométéores et processus microphysiques associés à la suppression de pluie verglaçante dans ce cas particulier sont décrits. Dans la cinquième, on aborde les impacts de l'introduction d'une température seuil de regel pour le gel par collision. Dans la sixième, les effets de la variation de l'efficacité de collecte sont présentés. La septième section contient les conclusions de cette étude et une discussion des résultats. Les tableaux et figures sont présentés la fin du chapitre II. Le chapitre III de ce mémoire, qui est rédigé en français, contient également une discussion des résultats et les conclusions qui en sont tirées. Les annexes et références sont présentés à la fin du mémoire.

CHAPTER II

LES IMPACTS DU GEL PAR COLLISION SUR LA PRODUCTION DE PLUIE VERGLAÇANTE

Ce chapitre, présenté sous forme d'un article rédigé en anglais, et prêt à être soumis, porte sur l'impact du gel par collision sur la prévision de pluie verglaçante dans un schéma microphysique à deux moments couplé avec un modèle de prévision numérique, plus particulièrement le Système à Haute Résolution de Prévisions numériques Déterministes (SHRPD) du Centre de Météorologique Canadien (CMC).

10

Impact of collisional freezing on the production of freezing rain

Agnieszka Barszcz[1,2], Julie Thériault [1], and Jason Milbrandt[2]

[1] *Université du Québec à Montréal*

[2] *Environnement et Changement climatique Canada*

Ready to submit to Atmospheric Research

March 11, 2017

ABSTRACT

Freezing rain events can have major consequences on road security and power networks. The processes leading to freezing rain are complex because it is associated with temperatures near 0°C. The types of precipitation formed at that temperature can interact among each other and lead to other types of precipitation while eliminating others. The accurate parameterization of freezing rain in numerical weather prediction models can be computationally expensive and therefore assumptions need to be made. The goal of this study is to investigate the role of collection and collision on the occurrence or elimination of freezing rain at the surface. A case study associated with a freezing rain severe under-prediction has been identified. On 24-25 December 2014, the Canadian High Resolution Deterministic Prediction System (HRDPS) had under-predicted the amounts of freezing rain, forecasting maximum amounts of 2 mm compared with observed amounts exceeding 20 mm in some areas in the province of Québec. A sensitivity study has been conducted over a small domain of the HRDPS using the Milbrandt and Yau (2005) microphysics scheme to investigate the conditions in which collisions and collection occurred during the storm. First, a temperature threshold for the occurrence of collisional freezing of drops has been introduced and its impacts have been investigated. Second, sensitivity tests were performed by systematically varying the collection efficiency between liquid and solid particles. It was shown that the collection of graupel with freezing rain has lead to the freezing rain under-prediction. Lower temperature thresholds and lower collection efficiencies led to higher freezing precipitation amounts. It was also shown that the collocated presence of small amount of solid

precipitation with freezing rain is sufficient to glaciate large amounts of water. To conclude, the temperature at which the freezing of liquid drops occurs when interacting with a frozen particle is critical. It can lead to the elimination of freezing rain at the surface. Accurate representation of the processes leading to freezing should be included into numerical models to better predict such precipitation types.

Key words: Freezing rain, ice pellets, graupel, collision, collision freezing, 3 component freezing

2.1 Introduction

Forecasting precipitation types during the winter season is critical because they can lead to major impacts on the society by affecting transportation and power networks. When covered with a coat of ice, roads become very slippery, and small aircrafts cannot safely fly. During the winter season, the environmental temperature often fluctuate around 0°C and many types of precipitation can be formed (Stewart, 1992). These can be liquid, solid as well as a mixture of both.

Ahead of the warm front, a temperature inversion can develop with a warm layer (> 0°C) aloft and a subfreezing layer near the surface (< 0°C). A schematic of a warm-front cross-section is depicted in Figure 2.1. Where the air temperature remains colder then 0°C, snow that has formed aloft will not melt when falling through the atmosphere. In the areas where the temperature inversion is slightly warmer then 0°C, snow gradually melts while falling within the warm layer. As it falls under the melting layer back into the subfreezing temperature layer, the remaining ice within the particles initiates the freezing and the particles refreeze into ice pellets before reaching the surface. This process is the primary source of ice pellets formation (Hanesiak and Stewart, 1995; Zerr, 1997). In areas where melting layer aloft is sufficiently deep and warm, all frozen particles melt completely and, in turn, do not refreeze in the cold layer. Rather, in the subfreezing layer, the liquid drops become supercooled, and only freeze upon entering with the sub-freezing surface to produce freezing rain. This is the classical freezing rain formation process (Pruppacher and Klett, 1997).

Climatological studies have shown that in the vicinity of the 0°C isotherm, many precipitation types, such as rain, freezing rain, ice pellets or snow can occur simultaneously or one after the other (Cortinas *et al.*, 2004). These precipitation types can all interact among each other and lead to other types, while

eliminating others (Stewart *et al.*, 2015). It has been shown through observational and theoretical studies that the collisional freezing of rain can be an important process and lead to reductions in freezing rain rates at the surface (Stewart and Crawford, 1995; Zerr, 1997; Gibson and Stewart, 2007). The microphysical processes leading to this process are complex (Stewart *et al.*, 2015), and the parameterization of these processes in various microphysical schemes is subtle but important to correctly forecast freezing rain.

In general, the hydrometeors that are completely melted upon entering the refreezing layer would not refreeze. An active ice nuclei has to be present to initialize the freezing of a water droplet. In the absence of a foreign substrate, water droplets will freeze at temperatures below $-38°C$. At this temperature, the statistical fluctuation of the water molecules can align to form an ice-like structure and initiate the freezing (Langham and Mason, 1958; Rogers and Yau, 1989; Pruppacher and Klett, 1997).

Ice nucleation can lead to the re-freezing of supercooled water drops at temperatures colder than $-5°C$ (Stewart and Crawford, 1995) because some ice nuclei can be activated at these temperatures. These liquid drops could either originate from the melting layer, or be formed through warm rain processes.

Furthermore, it is possible that ice particles are formed in situ in the refreezing layer through the deposition of water vapor on activated ice nuclei, given that the air temperature is cold enough ($-5°C$) (Meyers *et al.*, 1992; Stewart and Crawford, 1995; Zerr, 1997). However, this temperature varies as a function of the substrate, the size of the drop, the air temperature and supersaturation of the atmosphere. (Fletcher, 1958, 1969; Cooper, 1986; Meyers *et al.*, 1992). The Hallett-Mossop (1974) ice multiplication process also contributes to the freezing of water droplets. This secondary ice process can lead to the production of ice

crystals when the temperature is between $-8°C$ and $-3°C$ (Hallett, 1974). The locally produced ice crystals can interact with the supercooled drops and act as ice nucleis to initiate freezing. This process can lead, for example, to the production of ice pellets.

Once crystals are nucleated they may grow rapidly by water vapor diffusion, especially in the presence of supercooled water, as it is energetically more favorable for water to exist as ice rather than liquid when the air temperature drops below freezing. Thus the ice crystals grow at the expense of water droplets that evaporate. This is known as the Bergeron process (Bergeron, 1935; Rogers and Yau, 1989).

At temperatures above $-5°C$, the freezing of completely melted particles can be initiated by collisional freezing. Collisional freezing occurs when a supercooled liquid drop collides on a frozen hydrometeor. There exist many combinations of collisions. For example, a supercooled drop can collide with an ice pellets to form an ice pellet aggregate (Gibson and Stewart, 2007; Carmichael *et al.*, 2011). Furthermore, Carmichael *et al.* (2011) showed that most hydrometeors under a melting layer were not completely frozen upon reaching the ground. This means that if the ice shell is thin enough when it collides with another particle, it can break and produce an ice pellet aggregate. Also, these collisional freezing can lead to the elimination of freezing rain in the subfreezing layer near the surface (Stewart and Crawford, 1995; Carmichael *et al.*, 2011).

Collisions between hydrometeors may occur as a result of the combination of gravitational, electrical and aerodynamic forces. In clouds, the gravitational force dominates and the faster falling particles (the collectors) overtake the smaller ones (the collected particles). Only a fraction of the particles, that lie on the collector's path are collected, while the rest is swept aside in the airstream around the drop.

The fraction of collected particles depends on many factors such as particles sizes, shapes and densities. Once the particles enter into contact, they may coalesce or not. The product of the collision and the coalescence fractions is defined as the collection efficiency (Pitter and Pruppacher, 1974; Rogers and Yau, 1989; Cober and List, 1993; Khain *et al.*, 2001).

Once the freezing is initiated, drops freeze in three stages. The first stage is controlled through the internal rate of propagation of the ice within the drop. During the formation of ice, heat is generated. Very little of this heat is exchanged with the environment, and this stage lasts until the internal temperature of the drop has reached 0°C (Pruppacher and Klett, 1997). The fraction of the drop that freezes during this stage corresponds to approximatly $80/\Delta T$ where ΔT is the supercooling of the drop in degrees Celsius (Pruppacher and Klett, 1997). The freezing then continues with the semi-melted particle exchanging heat with its environment, through conduction and evaporation. During this stage the temperature of the drop remains equal to 0°C. The second stage takes a significantly longer time than the first stage (Pruppacher and Klett, 1997; Hindmarsh *et al.*, 2003). For example, it was shown in a theoretical study, that with an environment temperature colder then -2°C, only particles smaller than 2.5 mm would be completely frozen after traversing a 1000 m deep refreezing layer, given that little or no ice was initially present in the particle (Carmichael *et al.*, 2011). During the third stage, drops that are completely frozen, cool down to reach and equilibrium with their environement (Pruppacher and Klett, 1997; Hindmarsh *et al.*, 2003).

Numerical weather prediction (NWP) and research models typically represent cloud and precipitation formation and evolution using detailed microphysics parameterizations. There are several types of microphysics schemes, the main ones being the bin-resolving approach (Geresdi, 1998) and the bulk approach

(Ferrier, 1994; Thompson *et al.*, 2004; Hong and Lim, 2006; Milbrandt and Yau, 2005a,b). The bulk microphysics scheme uses an analytical size distribution where 1, 2 or 3 moments of the size distribution of each hydrometeor category can be predicted. For example, a double-moment microphysics scheme predicts the total number concentration and the mass-mixing ratio of each of the solid and liquid hydrometeors. These refer, respectively, to the 0^{th} and 3^{rd} moment of the size distribution with respect to diameter.

All the microphysical schemes allow for the collision of liquid and ice phase hydrometeors. The parameterization of this process varies from scheme to scheme. Many recent microphysics schemes parametrize collection through the Verlinde *et al.* (1990) equation (Ferrier, 1994; Reisner *et al.*, 1998; Cohard and Pinty, 2000; Milbrandt and Yau, 2005a,b; Straka and Mansell, 2005; Saleeby and Cotton, 2008). This equation is based on the assumption that all collisions are independent from each other and depend mainly on the size of the particles, their fall speed, and the collection efficiency factor (Appendix A). The resulting particle from collision freezing, also called three-component freezing, is determined using various methods, and depends on the complexity of the scheme. For example, Milbrandt and Yau (2005a) assumed that the nature of the resultant particle is determined according to the density of the resulting mean size of hydrometeor distribution. A large snowflake colliding with a small droplet will result in a larger snowflake, whereas a large supercooled raindrop colliding with a small snowflake will yield graupel or hail. On the other hand, Reisner *et al.* (1998) assumed that only a fraction of the resulting particles is transferred to the graupel category. Finally, in some schemes the particles transition through a mixed-phase category upon collision (Ferrier, 1994; Saleeby and Cotton, 2008).

The parameterization of the collection efficiency is treated differently by bulk

microphysics scheme. Some schemes such as Reisner *et al.* (1998), Milbrandt and Yau (2005a,b) and Straka and Mansell (2005) assumed a collection efficiency of 1 between raindrops and ice particles. Ferrier (1994) used a different collection efficiency depending upon whether the particle is wet or dry. Finally, Thompson *et al.* (2008) and Saleeby and Cotton (2008) parameterized the collection efficiency as a function of the collector and collected particle diameters using a bin scheme.

Given the importance of better understanding the formation mechanisms of freezing rain and how these interact with other types of precipitation, further investigations are needed. The goal of this study is to examine the impact of collisional freezing on the production of freezing rain at the surface. This will be achieved using the double-moment bulk microphysics scheme of Milbrandt and Yau (2005a,b), interfaced with the Global Environmental Multiscale (GEM) model. A particular case study associated with the elimination of freezing rain through collisional freezing will be presented. The sensitivity to the parameterization of the collisional freezing will be investigated systematically by varying the temperature threshold and the collection efficiency factor.

The paper is organized as follows. Section 2.2 summarizes the case study associated with the under-prediction of freezing rain. Section 2.3 describes the model used, the experimental design and the numerical simulations conducted. Section 2.4 demonstrates that the production of freezing rain depends on key microphysical processes parameterized in the bulk microphysics scheme. Section 2.5 shows the impact of the temperature threshold assumed for the refreezing of particles. Section 2.6 shows how the collection efficiency impacts the evolution and formation of freezing rain. Section 2.7 summarizes and concludes the study.

2.2 Case study

2.2.1 Synoptic conditions

On 24-25 December 2014, a low pressure system affected the province of Québec and the Maritimes (Canada) (Figure 2.2). While snow was forecast for some regions of the Québec by the operational High Resolution Deterministic Prediction System (HRDPS) model, high amounts of freezing rain were reported. Some initial analysis of the cause associated with this missed freezing rain forecast revealed that the representation of the interactions of hydrometeor could have been responsible. At 0000 UTC 24 December 2014, the 250 hPa level circulation was characterized by a relatively large-scale trough over the central plains of the United States and a ridge over New York state and Québec. As the day progressed the trough moved eastward, and a strong jet streak developed at that level. At the surface, a low pressure system over Alabama deepened during the day and progressed northeastward. Its development was supported by several factors. There was the upper-level divergence associated with the left exit region of the jet streak and positive vorticity advection at 500 hPa. Also, at 850 hPa, there was warm air advection in front of the low pressure system and cold air advection behind.

2.2.2 Reported precipitation types and amounts

The surface low pressure system produced a mixture of snow, freezing rain, rain, strong winds and thunderstorms over the Québec province (Figure 2.2). The total freezing rain amount and duration reported during this event are shown in Figure 2.3. The stations are listed in Table 2.1. The warm frontal system passed southern Ontario at 1200 UTC 23 December 2014. It produced 1 to 4 mm of freezing precipitation over the Montréal area in 3 h. The two stations that reported the most freezing rain were situated just north of the warm front.

These are Charlevoix (CWIS) and Matane (Gaspésie) and they reported 22 and 23 mm, respectively. Other stations reported on average between 1 and 15 mm of freezing rain (Figure 2.3). On average, the observations over the Quebec reported between 25-35 mm of rain (excluding freezing rain) between 23 and 25 December 2014. Stations in eastern Quebec (Gaspésie the Lower North Shore) reported up to 65 mm of rain. Regions in northern Quebec (La Grande-Rivière (CYGL) and Wabush (CYWK)) remained in the cold air during the passage of this system and received 15 and 30 cm of snow, respectively.

2.2.3 Model forecast of the storm

The storm of 24 December 2014 was simulated using the Regional Deterministic Prediction System (RDPS) (Mailhot *et al.*, 2006; Caron *et al.*, 2015) and HRDPS (Milbrandt *et al.*, 2016) operational models developed by Canadian Meteorological Centre (CMC) (See Section 2.3.1 for more details). The domains used for these simulations are shown in Figure 2.4. The 36 h accumulated precipitation and freezing rain are shown in Figure 2.5. Both models forecasted 15 to 30 mm of accumulated precipitation within 36 h with a similar spatial distribution. However, the RDPS and HRDPS showed very different freezing precipitation amounts and patterns (Figure 2.5). For example, the RDPS predicted 2.5 to 15 mm whereas the HRDPS predicted less than 2.5 mm. The RDPS generally predicted correctly the observed freezing rain quantities. None of the operational models have forecasted the high amount of freezing rain (>20 mm) received on the north shore of the St Lawrence River (Haute-Charlevoix (CWIS) and at Cap Chat (CWSG)). Overall, the RDPS reasonably predicted the freezing rain amounts, while the HRDPS generally under predicted freezing rain amounts over the entire region.

2.3 Experimental design

2.3.1 Model configuration

The two NWP models led to different types of precipitation and amounts over the Quebec province during the 24-25 December 2014 freezing rain event. The RDPS uses the Sundqvist (1988) condensation scheme to determine the precipitation amounts, combined with the Bourgouin (2000) method to diagnose the type of precipitation. On the other hand, the HRDPS uses the double-moment Milbrandt-Yau (2005) microphysics scheme (MY2) (Figure 2.6). As the HRDPS has a high computational cost due to its high spatial resolution and the storm has only affected the eastern portions of the HRDPS grid, a subdomain is used to carry out this study. This experiment will be used as a control run (CTR) as it is sufficient to reproduce the behavior of the full HRDPS (Appendix B). The domains of the RDPS, the HRDPS and the CTR run are shown in Figure 2.4.

The operational HRDPS is a high resolution model (2.5 km and 60 s time step), that runs on a 2560 x 1310 grid. It is a Limited Area Model (LAM) that is driven by the RDPS model with lateral boundary conditions every hour. It uses the ISBA (Noilhan and Planton, 1989) land surface scheme, the CCCmarad radiation schemes (Li and Barker, 2005), the Blackadar turbulent mixing length. Within the HRDPS clouds can be created in five ways: they can be initialized based on results from previous runs (wet start), created by the MY2 scheme, the shallow convection (Kuo-Transient), the deep convection (Kain and Fritsch, 1993), or the boundary layer scheme MoisTKE (Mailhot and Bélair, 2002).

MY2 is a double moment bulk microphysics scheme with six hydrometeor categories: cloud, rain, ice, snow, graupel and hail. The particle size distribution for each category is represented by a 3-parameter gamma function. The prognostic equations for the mixing ratio and the number concentration of

particles are the 3^{rd} and 0^{th} moment of that size distribution. All the particles are assumed to be spherical with constant bulk densities except for snow. The density of snow is assumed to decrease with the snow diameter as suggested in Brandes *et al.* (2007). The collection, conversion, freezing, ice multiplication, melting, nucleation, shedding and diffusional growth and sedimentation processes are represented (Milbrandt and Yau, 2005a,b).

2.3.2 Methodology

To show that the microphysics scheme is responsible for the freezing rain under prediction, the CTR run was reproduced with a different microphysics scheme. The MY2 scheme was replaced with the Sundqvist microphysics scheme and precipitation types were diagnosed using the Bourgouin (2000) technique (EXP1). Freezing rain amounts in EXP1 (Figure 2.7a) are different from the amounts in CTR (Figure 2.5d). They are similar to the observed amounts (Figure 2.3) and the RDPS run (Figure 2.5c). Thus it is possible to conclude that the missed forecast of freezing rain amounts by the HRDPS is due to the microphysical parameterization in the model.

To further narrow down the source of the freezing rain bust forecast, the precipitation types from the CTR run were processed using the Bourgouin (2000) technique (EXP2) (Figure 2.7b). The total freezing rain amounts are again closer to the EXP1 (Figure 2.7a) and the RDPS runs (Figure 2.5c). This shows that the problem does not lie in the amounts of precipitation that are forecast by the model but the type of precipitation predicted by MY2.

To get a better understanding of the causes of the under predicted freezing rain amounts forecasted using the MY2 scheme, a representative vertical cross-section through the warm front is chosen to examine precipitation types as well as the formulation of processes at the surface and aloft.

Many assumptions are behind the parameterization of collision freezing. It is assumed that the freezing of water droplets occurs at temperatures colder then 0°C, and that the collection efficiency between frozen and liquid particles is 1. The sensitivity of the freezing rain forecasts with respect to those two parameters will be investigated. To show that the three-component freezing is responsible for the missed freezing rain forecasts, the threshold temperature will be systematically varied from −9°C to 0°C (EXP3A-H). Then the collection efficiencies of rain-snow and rain-ice are going to be systematically varied while keeping the rain-graupel efficiency equal to 1 (EXP4A-E). Finally, the rain-snow and rain-ice collection efficiencies will be systematically varied while keeping the rain-graupel collection efficiency equal 1 (EXP5A-E) (See Table 2.2 for experiment names and furthur details). Results representing the freezing rain amounts, as well as the percentage reduction of freezing rain along a cross-section, and on the total domain will be analyzed. The next section shows that the collision freezing process is responsible for the freezing rain elimination during the 24-25 December 2014 event.

2.4 Hydrometeors and microphysical processes associated with the suppression of freezing rain

A vertical cross-section perpendicular to the warm front is examined to further investigate the bust of the HRDPS freezing rain forecast. It was chosen to be close to Cap Chat, Gaspésie (CWSG), where significant amounts of freezing rain were reported. It is also perpendicular to the 850 hPa isotherms. The cross-section is valid at 1800 UTC 24 December 2014 as at this time, the Gaspésie region was located under the warm layer. This cross-section is appropriate to study the distribution of hydrometeors and the modeled processes that lead to the presence of freezing rain under the melting layer. Its location is shown in Figure 2.8. Cross-sections of hydrometeor mixing ratios are shown in Figures 2.9 and 2.10. Both cloud and rain are mainly present within the melting layer. Cloud droplets

are present above the melting layer whereas rain is present under it. Under the melting layer, the rain mixing ratio decreases with lowering altitude to reach a very small amount at the ground. Significant amounts of rain are also present over the melting layer up to a temperature of $-2°C$, and trace amounts up to a temperature of $-30°C$. Although ice crystals and snow are mainly present above and ahead of the melting layer, there is an area under the melting layer where they are also present. Where the inversion is very thin, snow does not completely melt and will fall below the melting layer. Graupel is present ahead, over, in and under the melting layer. This suggests that both liquid and solid precipitation can exist simultaneously at the same location, which can lead to the formation of graupel. At the surface, under the inversion, precipitation is mainly composed of graupel, which accumulates at a rate of 1-3 mm h^{-1}.

Cross-sections representing the processes that lead to the suppression of freezing rain are presented in Figure 2.11. These are the 3 collisional freezing terms, which are rain-ice, rain-snow and rain-graupel. The most important term is the rain-graupel collision term: it is one order of magnitude larger than the other 2 terms. For example, at 1800 UTC 24 December 2014, the total rate of change of mixing ratio due to collisions over the entire domain is 5×10^{-2} kg $kg^{-1}s^{-1}$ for rain-graupel collisions, 5×10^{-3} kg $kg^{-1}s^{-1}$ for rain-snow collisions and 8×10^{-4} kg $kg^{-1}s^{-1}$ for rain-ice collisions for the CTR experiment. Therefore, the collisional freezing of rain-graupel is the dominant collisional freezing term during this event. It could be the process responsible of the freezing rain elimination during the 24-25 December 2014 event.

The next two sections focus on experiments that were done in order to better understand the role of collisional freezing on the production of freezing rain. The first one (Section 2.5) focuses on the introduction of a temperature threshold for collisional freezing, and the second one (Section 2.6) focuses on the variation of

the collection efficiency between solid and liquid hydrometeors.

2.5 Temperature threshold sensitivity test

In this section, we will investigate the effects of the temperature threshold at which the liquid precipitation is being collected by solid precipitation. The temperature threshold used to simulate collisional freezing is not a physical limit but rather a surrogate for something physical that is difficult to parameterize within the limits and specifications in the MY2 bulk microphysics scheme. This is because this scheme does not track the temperature of the particle and in reality the temperature of falling drops is not necessary equal to the surrounding air temperature. The drops temperature is the result of the latent and sensible heat fluxes between the particle and its environment. The temperature of mixed-phase particle is 0°C but this is not the case for pure liquid or solid particles. When supercooled drops fall in a refreezing layer near the surface, their temperature will likely increase because they take some time to cool after falling through the melting layer above it. Because liquid drops have a high terminal fall velocity (5 m s^{-1}), they may fall a long distance before reaching an equilibrium temperature with their environment. Therefore, they may not be supercooled when the air temperature is slightly below the freezing point. It is therefore very difficult to model precisely the temperature of a liquid drop falling through the atmosphere. This is different for colder drops ($T < -15$°C) mainly because the probability for ice nuclei to be activated is higher (Pruppacher and Klett, 1997). Also, there is no partially-melted snow category in MY2, creating a general deficiency in the scheme's ability to model precipitation types when the temperature is near 0°C. So there is a physical basis for imposing a temperature threshold < 0°C to allow collisional freezing to occur. This is simply a crude parameterization of a physical process.

The production of freezing rain by collisional freezing at the surface has been investigated. Figure 2.12 shows the percentage of precipitation represented by freezing rain, graupel, and their sum along the cross-section for various temperature thresholds. Under the melting layer, 90% of the precipitation is composed of freezing rain and/or graupel (Figure 2.12a), the rest is composed of snow and ice crystals. The area associated with freezing rain increases with increasing the threshold temperature (Figure 2.12b). With a threshold temperature colder than -5°C, significant amounts of graupel are only present on an area smaller than 30 km and represent less than 70% of the total precipitation rate (Figure 2.12c). This corresponds to the area where the warm layer is shallowest, with a maximum temperature close to 0 °C. It also corresponds to the region where the air temperature in the refreezing layer is the coldest, i.e.,-5.8°C (Figure 2.12d).

Very little amount of graupel ($<$ 10% of the total precipitation rate) is present with freezing rain. Figure 2.12b shows that small amounts of graupel ($<$ 10% of total precipitation) are still present in areas where the collisional freezing is suppressed through a threshold temperature. This demonstrates that the presence of small amounts graupel is sufficient to reduce significantly (eliminate) the forecasted amounts of freezing rain through a collisional freezing process due to excessive glaciation.

Freezing rain can be formed in various ways in the atmosphere, though warm and cold process. Rain and ice particles can thus coexist outside of the refreezing layer, and collision freezing processes are therefore not restricted to occur within this layer. For example, in our experiment, trace amounts of supercooled water are found with an environement temperature of -30°C. We therefore compare the effects of a threshold temperature for collision freezing with and without a melting layer. Figure 2.13 shows the domain-integrated mean precipitation rates

and surface areas of freezing rain and graupel as a function of the temperature threshold. A trend of increasing (decreasing) precipitation rate of freezing rain (graupel) and surface area with a decreasing temperature threshold is shown. The results are broken down according to the presence or absence of a melting layer in the vertical temperature profile above a grid point. Over the entire domain, 88% (95%) of the freezing rain precipitation is located under the melting layer with a temperature threshold of 0°C (-9°C). The area of freezing rain under the melting layer represents 16% (20%) of the area affected by freezing rain with a temperature threshold of 0°C (-9°C). Furthermore, 60% (22%) of graupel precipitation rate is located under the melting layer with a temperature threshold of 0°C (−9°C). The area of graupel under the melting layer represents 13% (14%) of the area affected by freezing rain at with a temperature threshold of 0°C (-9°C). This confirms that freezing rain and graupel are present and can interact outside of the melting layer aloft. However, the effects of a temperature threshold outside of the melting layer are minimal, as most of the supercooled liquid water is found under the melting layer.

The temperature threshold condition has a more significant impact on the freezing rain precipitation rates at warm temperatures than at cold temperatures (Figure 2.14). The variation of freezing rain rates at the surface as a function of temperature thresholds shows a plateau at cold temperature thresholds. For example, the difference between the domain-integrated total freezing rain amounts between the experiments with a threshold temperature of 0°C and -1°C is 0.6 kg kg^{-1}, whereas between the experiments of -7°C and -9°C is much less (0.01 kg kg^{-1}). This is explained by the fact that there are more supercooled rain droplets present in the atmosphere at warmer temperatures, than at cold temperatures. The domain-integrated total mixing ratios of supercooled liquid rain and graupel whithin isothermal atmospheric layers, are shown in Figure

2.14. The amount of supercooled liquid water decreases with decreasing air temperature. This is true for all experiments, regardless of the collision freezing threshold temperature. Finally, as the threshold temperature decreases the amount of supercooled liquid water and graupel increases. At warm air temperatures, there is more available supercooled liquid water for riming and collision freezing processes, which are two sources of graupel particles.

Overall large amounts of freezing rain can be suppressed through excessive collisional freezing. In our expermiment, over 90% of the precipitation is glaciated because this process. This is more then the maximum 60% reduction, which was previously suggested by Carmichael *et al.* (2011) based on a theoretical study. This process can be controlled by imposing a lower temperature threshold (e.g. -5°C) that simulates a drop freezing at colder air temperatures as reported in laboratory studies (Hindmarsh *et al.*, 2003). Finally, the collisional freezing is mainly active under the melting layer and acts to suppress freezing rain at the surface especially at temperatures near 0°C. The next section shows the sensitivity of the forecast of freezing rain on the collection efficiency.

2.6 Collection efficiency sensitivity tests

In this set of experiments (EXP4 and EXP5), the impact of the collection efficiency is examined. In bulk schemes such as MY2, there are generally three collisional freezing terms, which are rain-ice, rain-snow, and rain-graupel. The first two terms do not require graupel to be present, whereas the third term only acts to enhance the amount of existing graupel. This set of sensitivity tests was conducted in two steps. First, E_{rs}, and E_{ri} were equal to 1, while E_{rg} was varied systematically (EXP4). In the second set of experiments, the collection efficiencies of rain-snow (E_{rs}) and rain-ice (E_{ri}) collisions were systematically varied, while keeping the

rain-graupel efficiency (E_{rg}) equal to 1 (EXP5). The percentage variation of precipitation at the surface, along the cross-section, for various rain-snow and rain-ice collection efficiency values, shows that these two terms have no significant effect on the surface precipitation rates (Figure 2.15).

The percentage variations of precipitation at the surface, along the cross-section, for various rain-graupel collection efficiencies are shown in Figure 2.16. The larger the rain-graupel collection efficiency, the narrower (wider) is the area of freezing rain (graupel) at the surface. For this cross-section, a collection efficiency of 0.4 allows freezing rain to reach the surface. Once it does, freezing rain represents over 90% of the total precipitation reaching the surface. This result is specific to the location of this cross-section. If the cross-section was located at another location, this threshold would be different. The ice and snow precipitation rates are very small compared to the other precipitation types under the inversion ($< 1\%$ for ice, and $< 30\%$ for snow). The ice category exhibits a small variation as a function of the rain-graupel collection efficiency. This is because the rain-graupel collisions transform supercooled rain droplets into graupel. As a result, less rain is available to collide with ice. A higher rain-graupel collection therefore favours a higher ice precipitation rate under the melting layer.

To verify that these results can be generalised over the domain, the total accumulated amounts of freezing rain that fell between 0000 UTC 24 December 2014 and 1800 UTC 24 December 2014 are shown in Figure 2.17. The total surface area that received freezing rain is shown in Figure 2.18. Over the entire domain, the variation of the rain-graupel collection efficiency (E_{rg}) has a significant impact of the accumulated freezing rain amounts and surface area that was affected by freezing rain. The higher (lower) the collection efficiency, the lower (higher) are the freezing rain accumulations, and the smaller (larger) is the affected surface area. However, the variation of the ice-rain, and snow-rain

(E_{rs}, E_{ri}) collection efficiencies has little impact on the accumulation of freezing rain, nor on the total surface area.

Overall, these results show that for this case study, with the MY2 scheme, the forecasted freezing rain amounts are very sensitive to the rain-graupel three-component freezing term, but not to the rain-ice and rain-snow three-component freezing terms. Also, the greatest impact of the collection efficiency is under the melting layer because most of the freezing rain is located in this area. Finally, varying the rain-graupel collection efficiency has an impact on the amount of ice and snow particles present under the melting layer, although these amounts only account for small precipitation rates at the surface.

2.7 Discussion

We have identified a case where freezing rain was under-predicted by the HRDPS interfaced with the MY2 bulk microphysics scheme. We have further shown that the under-prediction was primarily due to the precipitation typing predicted in MY2 microphysics scheme. In fact, the MY2 scheme forecasts a similar precipitation amount as the Sundqvist condensation scheme, but the amount of precipitation in the freezing rain category is underestimated compared to observations and to the amount diagnosed using the Bourgouin method.

The threshold temperature for collisional freezing within MY2 scheme was systematically varied, and we have shown it has a significant impact on the forecasts of freezing rain amount. A small amount of graupel is sufficient to trigger the collisional freezing cascade of a large amount of freezing rain. Collisional freezing has a more important impact at warmer temperatures than at cold temperatures. This mainly affects the amount of freezing rain found under the melting layer where most supercooled drops are located. The collection efficiency was also systematically varied for the graupel enhancing

collisional freezing terms (rain-graupel) and graupel generating terms (rain-snow and rain-ice terms). It was shown that the rain-graupel collisional freezing term has the most important impact on the freezing rain amount and that the processes producing graupel have a negligible impact on the forecast freezing rain amount.

These results showed that the collisional freezing of supercooled rain is a very fast process. We have suggested that this may be due to the fact that the particles temperature is not necessary equal to the environment temperature as it is usually assumed in bulk microphysics schemes. Particles may be warmer than the environment, as the surrounding environment temperature falls below the freezing mark. Another assumption made in most bulk microphysics schemes is that the freezing of liquid particles is instateneous. Laboratory studies (Hindmarsh *et al.*, 2003) have shown that in nature, the freezing of liquid droplets is quick but not instantaneous. In fact, the initial crystal growth, which brings the particles temperature to the freezing point is extremely rapid but the second stage of freezing, during which the particles temperature is steady near the freezing mark, takes longer. The freezing time depends on the air temperature and the properties of the particle. For example, once the crystal growth is initiated, it would take about 30 s for a 2 mm drop to completely refreeze, if the environement temperature is $-15°C$, and the wind speed is 0.5 m s^{-1} (Hindmarsh *et al.*, 2003).

In nature, at temperatures close to 0°C, collisional freezing does not lead to complete freezing of particles, but rather to the formation of mixed-phase particles. The collisional freezing of droplets just above the warm layer can therefore create mixed-phase particles. As these fall through the warm layer, they melt faster compared to frozen particles of the same size because they contain less ice. In bulk microphyscic schemes, the assumption of instant

freezing upon a collision could have an impact on the melting time of particles formed just above the melting layer. In turn, this could increase the amount of ice particles traversing the warm layer without completely melting. This could theoretically affect the amount of ice phase particles available for collisional freezing in the refreezing layer.

Also most bulk microphysics schemes do not take into account semi-melted particles, which increases the chances of collisions between particles in the refreezing layer. In nature, the melted liquid water usually remains in the ice particle (Mitra *et al.*, 1990). In schemes such as MY2, when ice particles melt, the liquid fraction of the particle is instantly shed from the distribution. In the presence of a melting layer, this implies that semi-melted particles are split into two separate categories within the melting layer. This increases the chances of ice and liquid particles collisions in the refreezing layer as both of these particles have different terminal fall velocities. Thus, the absence of a semi-melted category theoretically increases the chances of occurrence of collisional freezing.

Another interesting characteristic of the representation of collisional freezing in bulk microphysics schemes, is that they conserve the mean particle mass of the particles during the interactions between solid and liquid particles rather than the number concentration of particles. The number concentration of particles is directly used in the calculation of the number of collisions. Therefore, the impact of a different parametrization of changes in number concentration due to collisional freezing could be investigated.

In the absence of the representation of semi-melted particles, a temperature threshold of $-5°C$ should be applied to limit the impact of collisional freezing terms on the freezing rain amounts. In the vicinity of the freezing mark, it is very difficult to parameterize accurately the temperature of the particle.

Limiting the collection efficiency between rain and graupel could also slow down the collisional freezing processes. During this storm this collection efficiency should be set to zero for the freezing rain forecast to be closest to the observations.

Finally, the conclusions of this study are very specific to this storm. However, an under prediction of freezing rain amounts by the HRDPS was noted during other storms during the 2014-2015 winter. Similarly to our case study, large differences in the forecasted amount of freezing rain between the RDPS and HRDPS models were noted. For example a difference of 10 mm in forecast freezing rain amount was noted during the storm of 11-12 November 2014 over Ontario and Quebec, a 10 mm difference during the storm of 29 September 2015 over New Brunswick, and a 5 mm during the storm of 14 October 2015 over northern Quebec. It is reasonable to assume that the results and conclusions of this study would generally be valid for other storms since a temperature threshold of $-5°C$ for collisional freezing has been implemented in the operational HRDPS at CMC in December 2015 and it has been reported by operational meteorologists that this led to an improvement in the freezing rain forecasts during the 2015-2016 winter by this model.

Further investigations should be conducted. The impact of semi-melted particles on the collisional freezing processes and on the suppression of freezing rain could be explored. This would allow representing the freezing of particles as a gradual process. It would also allow exploring the impacts of the parameterization of the changes in number concentration of particles during solid-liquid interactions. It was already shown using a column model with the MY2 scheme that this could significantly impact precipitation types reaching the surface (Thériault and Stewart, 2010). Including such particles in a three dimensional NWP model could lead to improved forecasts of precipitation types when the temperature is near $0°C$. Finally, the implementation of a semi-melted category would allow and

improve the prediction of ice pellets.

2.8 Concluding remarks

The goal of this study was to better understand the impact of collisional freezing on the production of freezing rain. To do so, we have used the MY2 microphysics scheme coupled with the GEM model to simulate the freezing rain storm that has occurred on 24-25 December 2014 over eastern Canada. We have shown that the freezing rain amounts forecast by this model were insufficient due to the representation of collision freezing in the microphysics scheme. We have introduced a temperature threshold for collisional freezing, and modified the collection efficiency for collisional freezing terms. We have furthur shown that the production of freezing rain by two moment bulk schemes is sensitive to the presence of ice particles aloft. Small amounts of ice particle such as graupel or snow can lead to the elimination of freezing rain at the surface. This can be controlled by adding a temperature threshold for collisional freezing (e.g. -5°C) or by lowering the collection efficiency values.

Overall, this study contributes to better understand the importance of accounting for the key microphysical processes leading to the many types of precipitation produced when the temperature is near 0°C. In particular it is important to carefully choose the parameterization of collisional freezing, as it can significantly impact the forecast of freezing rain.

TABLES

Table 2.1: Name, code and province of the stations that report quantities or types of precipitation used in this study.

Station name	Station code	Province
Chibougameau	CYMT	Québec
Sherbrooke	CYSC	Québec
Québec	CYQB	Québec
Valcartier	CYOY	Québec
Charlevoix	CWIS	Québec
Bagotville	CYBG	Québec
Roberval	CYRJ	Québec
Edmunston	ERM	Québec
Mont-Joli	CYYY	Québec
Baie-Comeau	CYBC	Québec
Cap Chat	CWSG	Québec
Sept-Iles	CYZV	Québec
Havre-Saint-Pierre	CYGV	Québec
Gaspé	CYGP	Québec
Bathurst	CZBF	New Brunswick
Moncton	CYQM	New Brunswick
Fredericton	CYFC	New Brunswick
Greenwood	CYZX	New Brunswick
Halifax	CYHZ	New Brunswick

Table 2.2: List of runs

Experiment	Description, List of changes with respect to the control run
CTR	Downscaling of the full HRDPS model to an experimental grid
EXP1	Sundqvist microphysics and Bourgouin precipitation types
EXP2	MY2 microphisics and Bourgouin precipitation types
EXP3A	Threshold freezing temperature for collisional freezing = 0°C
EXP3B	Threshold freezing temperature for collisional freezing = −1°C
EXP3C	Threshold freezing temperature for collisional freezing = −2°C
EXP3D	Threshold freezing temperature for collisional freezing = −3°C
EXP3E	Threshold freezing temperature for collisional freezing = −4°C
EXP3F	Threshold freezing temperature for collisional freezing = −5°C
EXP3G	Threshold freezing temperature for collisional freezing = −7°C
EXP3H	Threshold freezing temperature for collisional freezing = −9°C
EXP4A	E_{rg}=0.8, E_{ri}=E_{rs}=1
EXP4B	E_{rg}=0.6, E_{ri}=E_{rs}=1
EXP4C	E_{rg}=0.4, E_{ri}=E_{rs}=1
EXP4D	E_{rg}=0.2, E_{ri}=E_{rs}=1
EXP4E	E_{rg}=0, E_{ri}=E_{rs}=1
EXP5A	E_{rg}=1, E_{ri}=E_{rs}=0.8
EXP5B	E_{rg}=1, E_{ri}=E_{rs}=0.6
EXP5C	E_{rg}=1, E_{ri}=E_{rs}=0.4
EXP5D	E_{rg}=1, E_{ri}=E_{rs}=0.2
EXP5E	E_{rg}=1, E_{ri}=E_{rs}=0.0

FIGURES

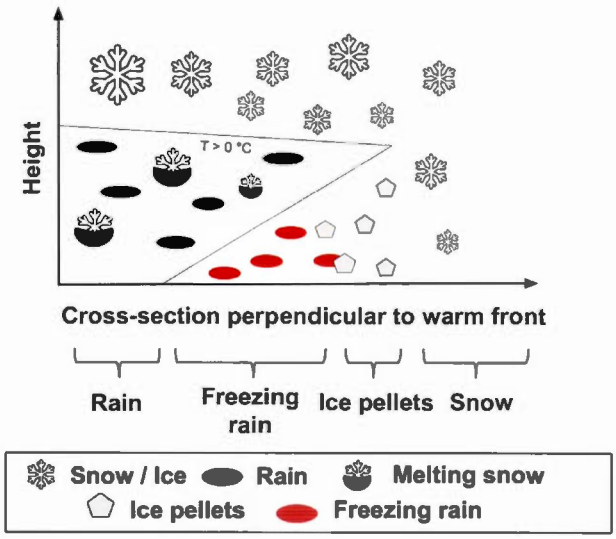

Figure 2.1: Typical cross-section of a precipitation type transition region associated with a warm front.

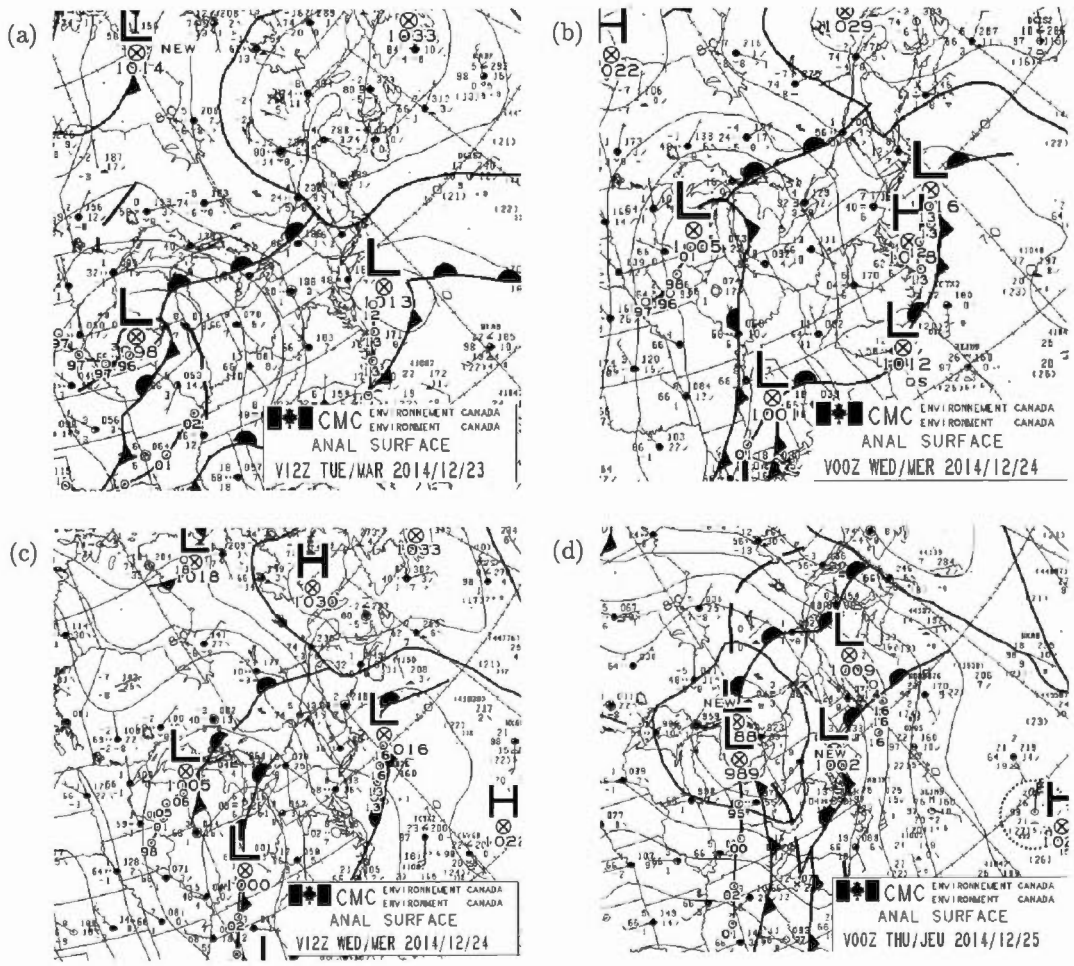

Figure 2.2: The surface analysis as issued by the Canadian Meteorological Center (CMC) valid at (a) 1200 UTC 23 December 2014, (b) 0000 UTC 24 December 2014, (c) 1200 UTC 24 December 2014 (d) 0000 UTC 25 December 2014.

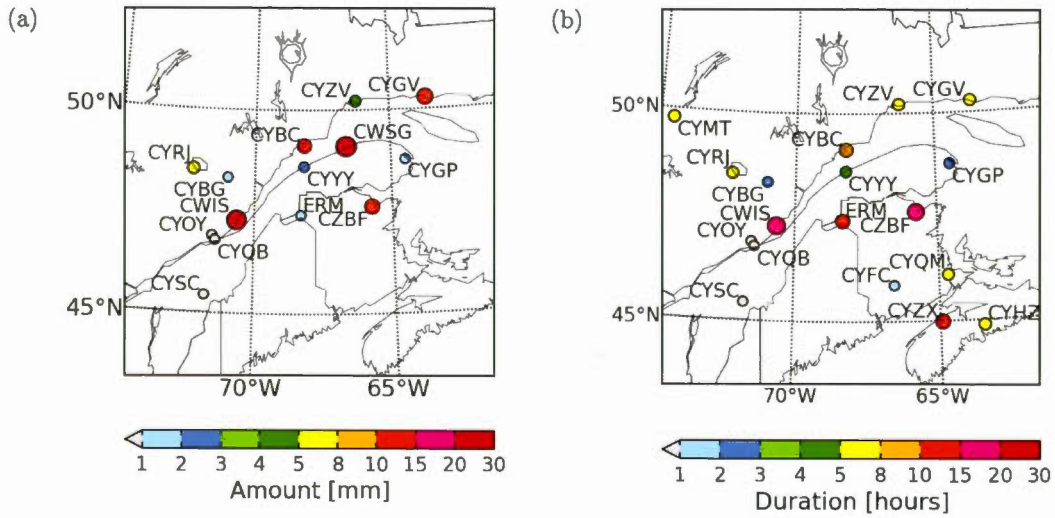

Figure 2.3: Observed (a) amounts (mm) and (b) durations (h) of freezing rain from 23 to 25 December 2014.

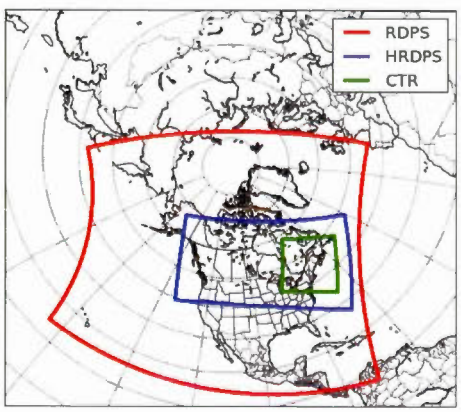

Figure 2.4: Geographic locations of the domains used to run the a) Regional Deterministic Prediction System (RDPS), b) High Resolution Deterministic Prediction System (HRDPS), as well as c) the domain for the the control (CTR) and sensitivity simulations (Table 2.2).

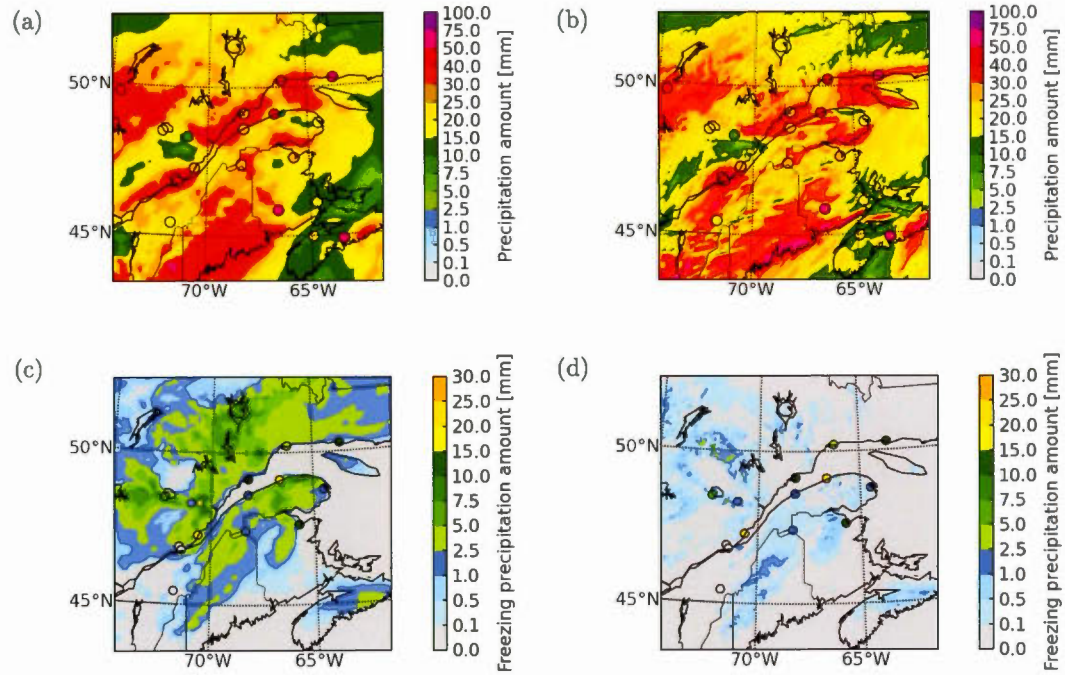

Figure 2.5: Comparison of 36 h accumulated precipitation (mm) forecast by the (a) Regional Deterministic Prediction System (RDPS) and (b) High Resolution Deterministic Prediction System (HRDPS). (c) and (d) are total freezing rain amounts forecast by the RDPS and HRDPS, respectively. The 36 h period starts 0000 UTC 24 December 2014 and finishes 1200 UTC 25 December 2014. The colored dots represent observed precipitation amounts.

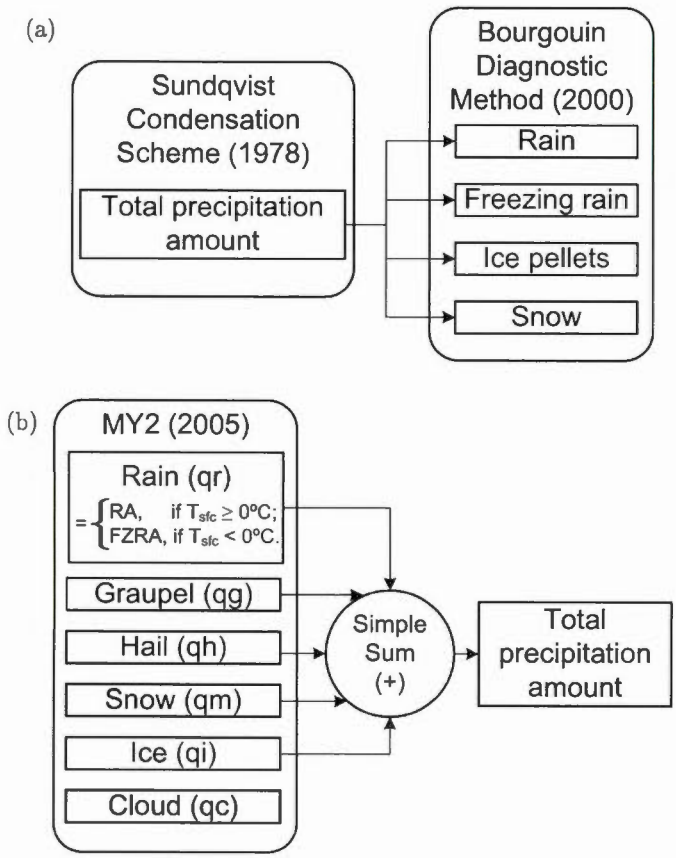

Figure 2.6: Schematic of the method used to determine the precipitation types and total precipitation amounts in the (a) Regional Deterministic Prediction System (RDPS), and (b) High Resolution Deterministic Prediction System (HRDPS). RA and FRZA are rain and freezing rain respectively. T_{sfc} is the surface air temperature.

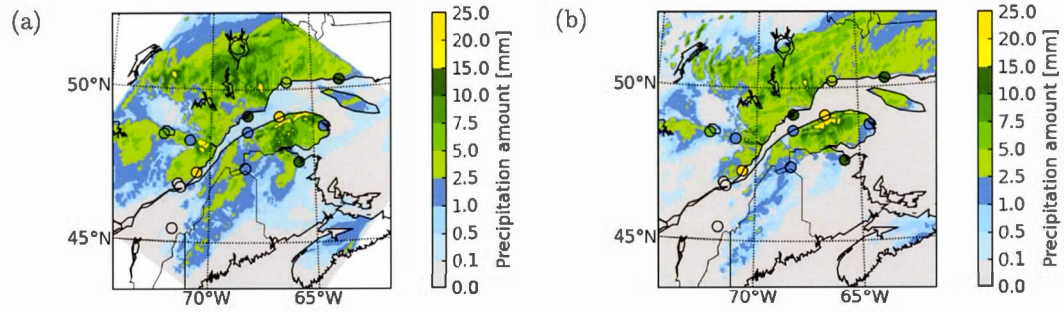

Figure 2.7: Comparison of the T+36 hours accumulation of freezing rain valid 1200 UTC 25 December 2014 from (a) EXP1 and (b) EXP2 runs (Table 2.2). Colored dots represent observed freezing rain amounts.

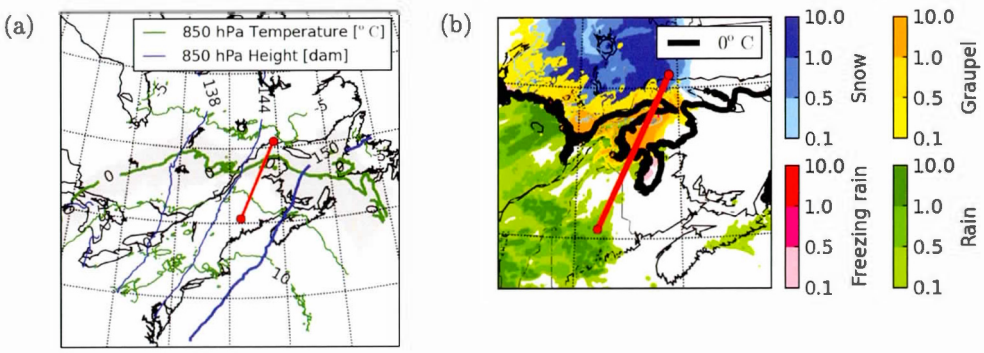

Figure 2.8: (a) 850 hPa geopotential height and temperature fields and (b) surface precipitation rates with the surface 0°C isoterm from CTR run (Table 2.2) valid at 1800 UTC 24 December 2014. The red line represents the location of the cross-section.

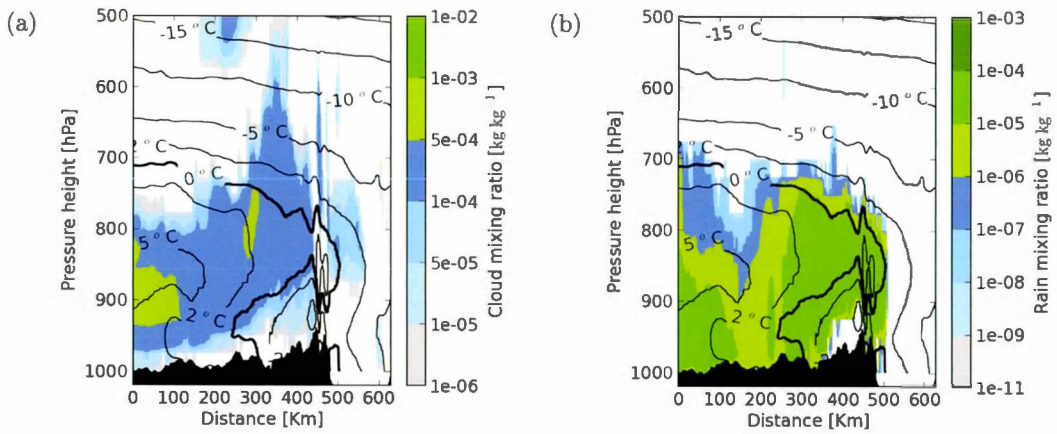

Figure 2.9: Vertical cross-sections of (a) cloud and (b) rain mixing ratios (kg kg^{-1}) from the CTR run along the cross-section shown in Figure 2.8, valid at 1800 UTC 24 December 2014. The black contour lines are isoterms (°C). The cross-section is approximately oriented from south-west (left) to north-east (right).

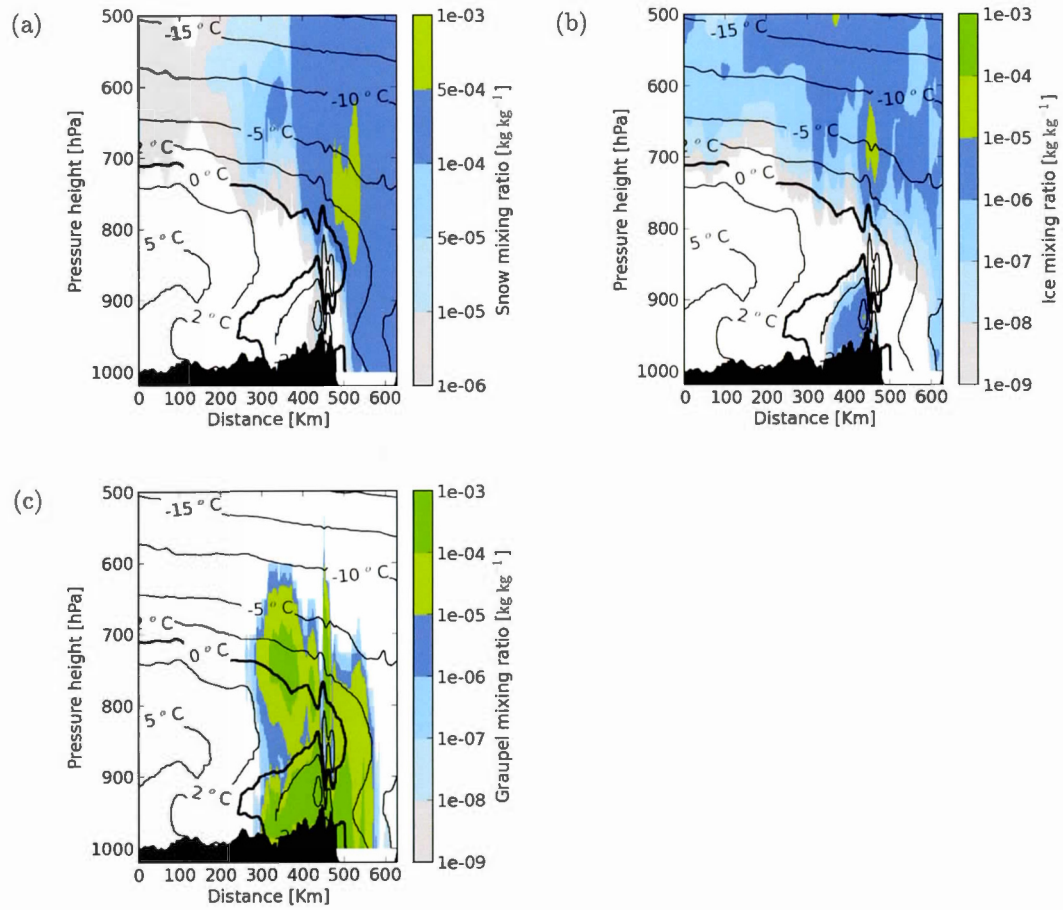

Figure 2.10: Vertical cross-sections of (a) snow (b) ice and (c) graupel mixing ratios (kg kg^{-1}) from the CTR run along the cross-section shown in Figure 2.8, valid at 1800 UTC 24 December 2014. The black contour lines are isotherms (°C). The cross-section is approximately oriented from south-west (left) to north-east (right).

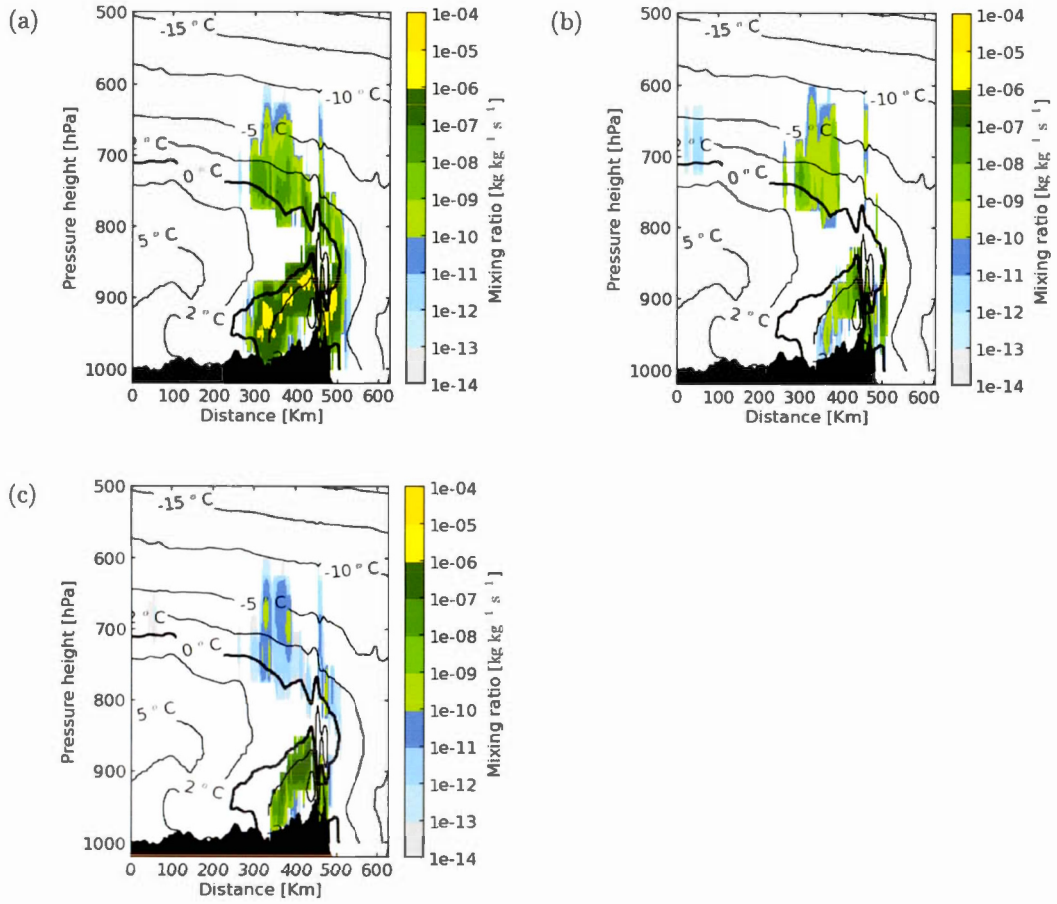

Figure 2.11: Vertical cross-sections of collision freezing terms from the CTR run valid at 1800 UTC 24 December 2014. Rate of change of mixing ratio between hydrometeor categories due to collisions between (a) rain-graupel (b) rain-snow (c) rain-ice (kg $kg^{-1}s^{-1}$). The black contour lines are isoterms (°C). The cross-section is approximately oriented from south-west (left) to north-east (right).

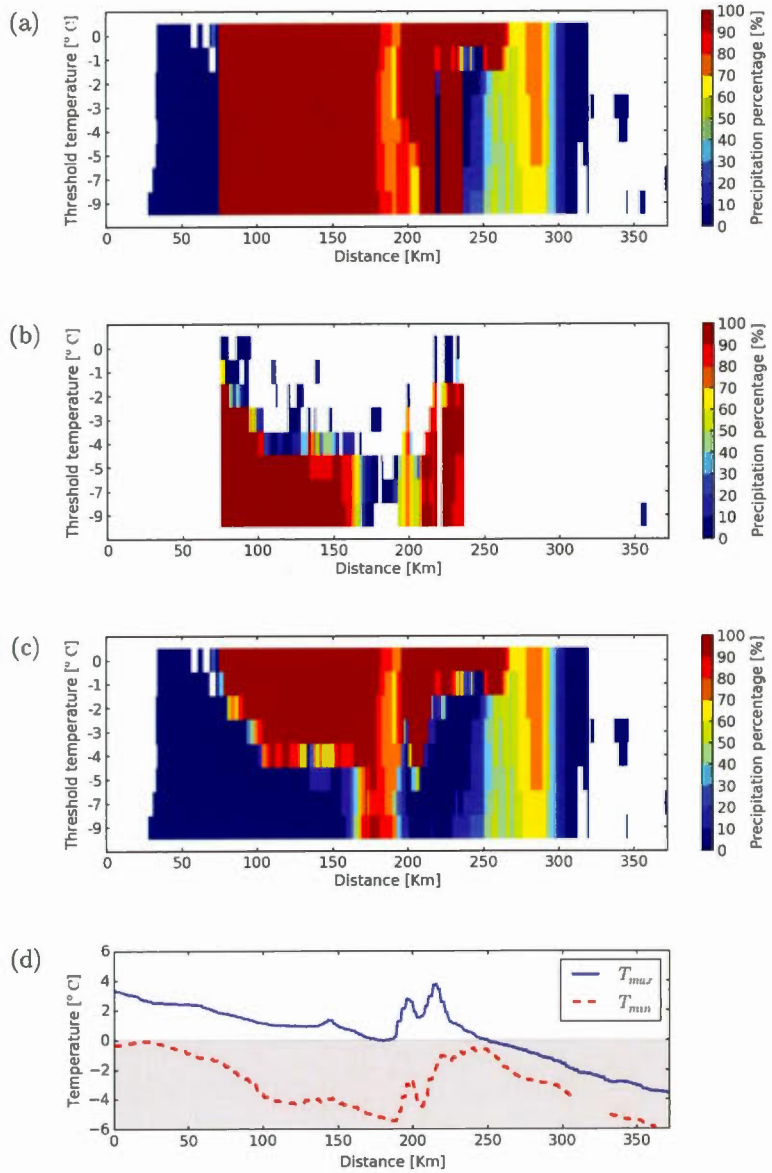

Figure 2.12: Percentage of instant precipitation rate represented by (a) the combination of freezing rain and graupel, (b) freezing rain only and (c) graupel, as function of the collisional freezing temperature threshold, along the vertical cross-section. (d) The maximum temperature of the air aloft (T_{max}) and the minimum air temperature below the inversion layer (T_{min}) along the cross-section. The cross-section is valid at 1800 UTC 24 December 2014 and approximately oriented from south-west (left) to north-east (right).

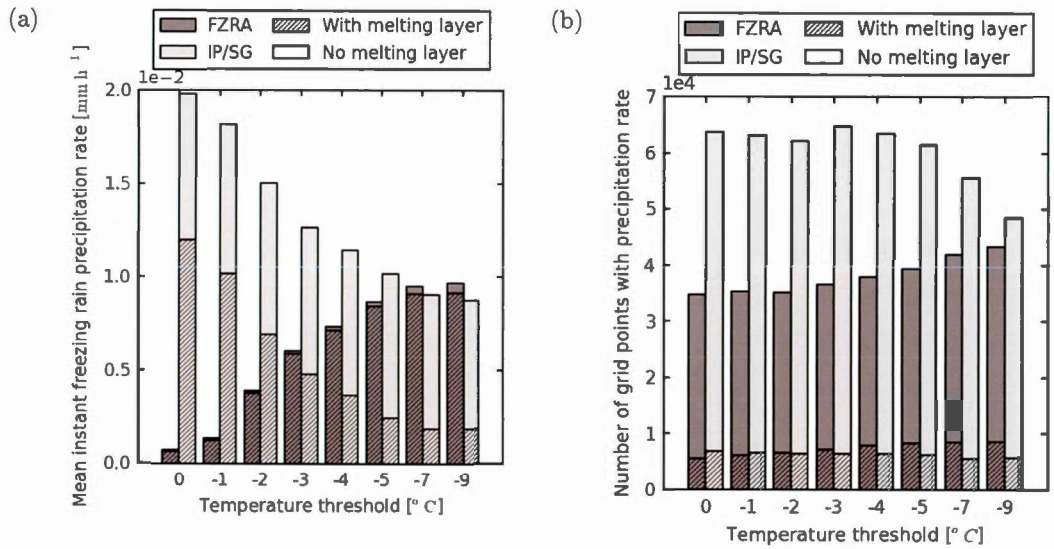

Figure 2.13: Domain-integrated (a) mean precipitation rates, and (b) number of grid-points receiving freezing rain (FZRA), ice-pellets (IP), and graupel (SG), valid 1800 UTC 24 December 2014, as a function of a temperature threshold. Results are stratified for grid-points associated with and without a melting layer aloft.

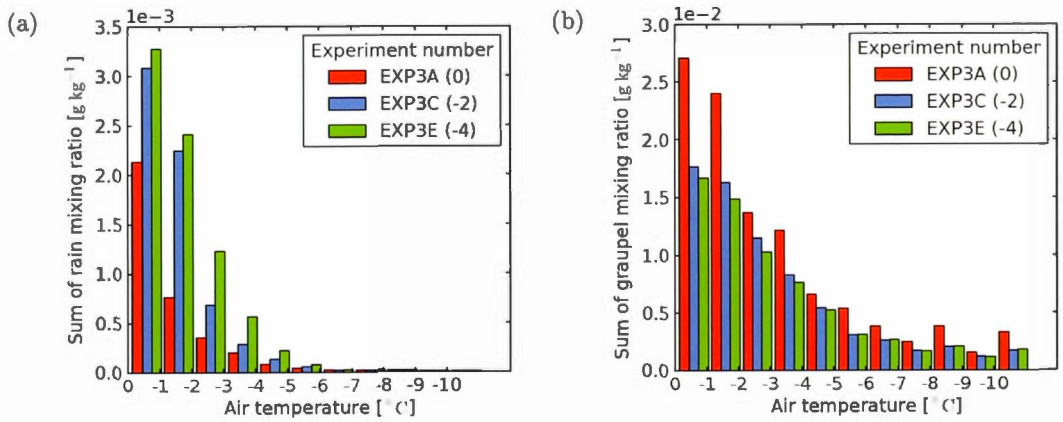

Figure 2.14: Domain-integrated total amounts of mixing ratio (kg kg^{-1}) of (a) supercooled liquid water and (b) graupel located within isothermal layers of the atmosphere. The results are shown for three experiments (Table 2.2) with various temperature thresholds for collisional freezing, valid at 1800 UTC 24 December 2014.

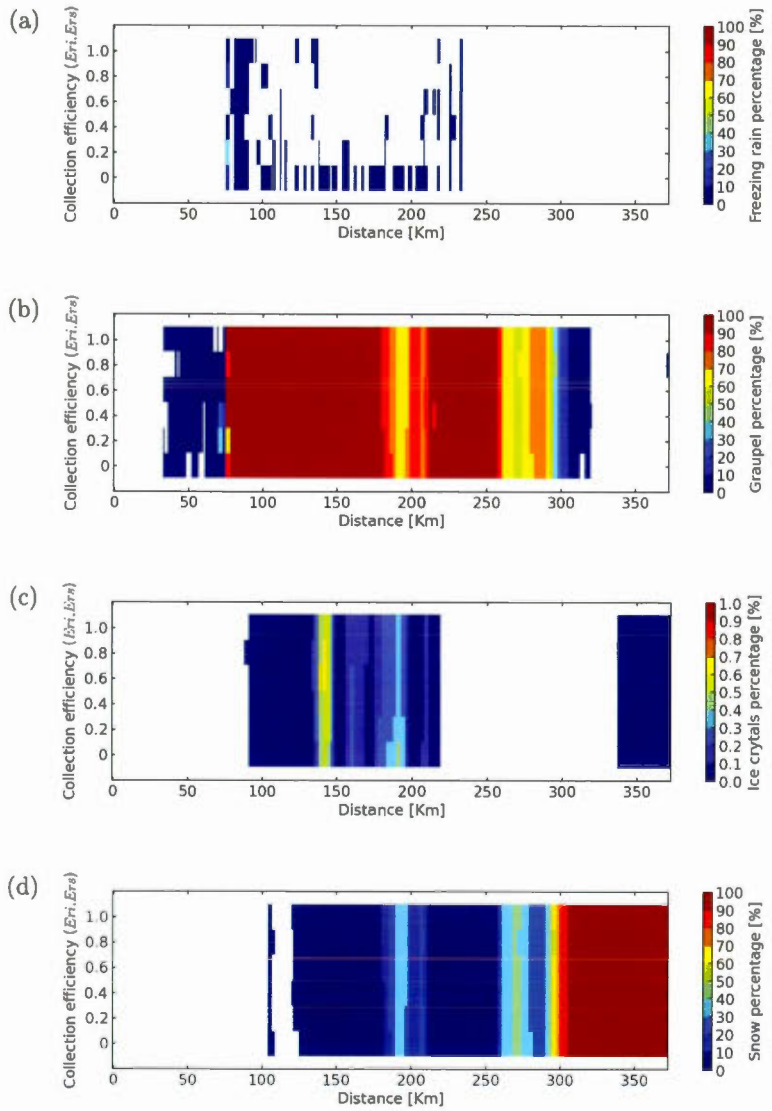

Figure 2.15: (a) Freezing rain, (b) graupel, (c) ice crystals and (c) snow percentage of instant precipitation rate as a function of the collection efficiency of rain by ice and snow (E_{ri}, E_{rs}) along the cross-section valid at 1800 UTC 24 December 2014. The cross-section is approximately oriented from south-west (left) to north-east (right).

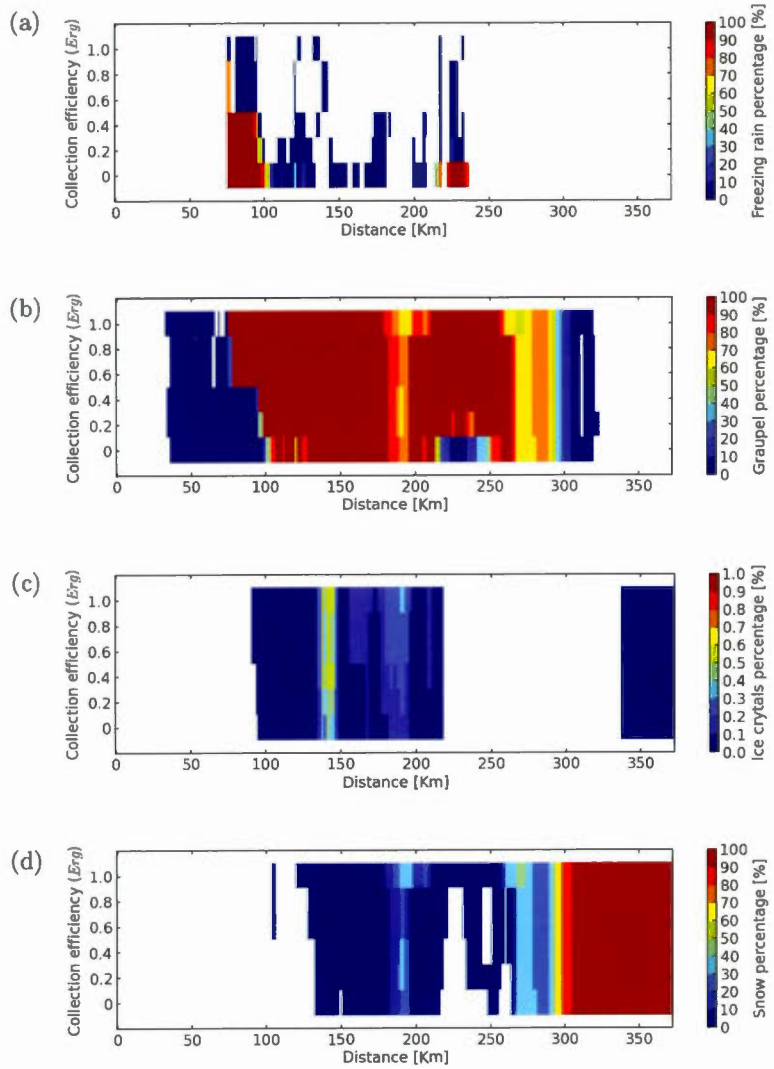

Figure 2.16: (a) Freezing rain, (b) graupel, (c) ice crystals and (c) snow percentage of instant precipitation rate, as a function of the collection efficiency of rain by graupel (E_{rg}), along the cross-section, valid at 1800 UTC 24 December 2014. The cross-section is approximately oriented from south-west (left) to north-east (right).

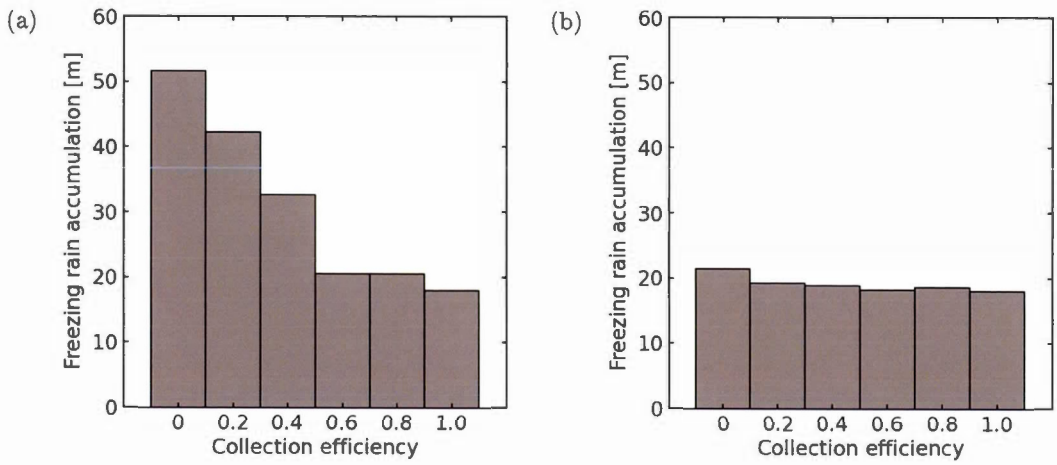

Figure 2.17: Freezing rain accumulation integrated over the domain from 0000 UTC 24 December 2014 to 1800 UTC 24 December 2014. (a) E_{rg} is systematically varied while E_{ri}, $E_{rs} = 1$ (b) $E_{rg} = 1$, while E_{ri} and E_{rs} are systematically varied.

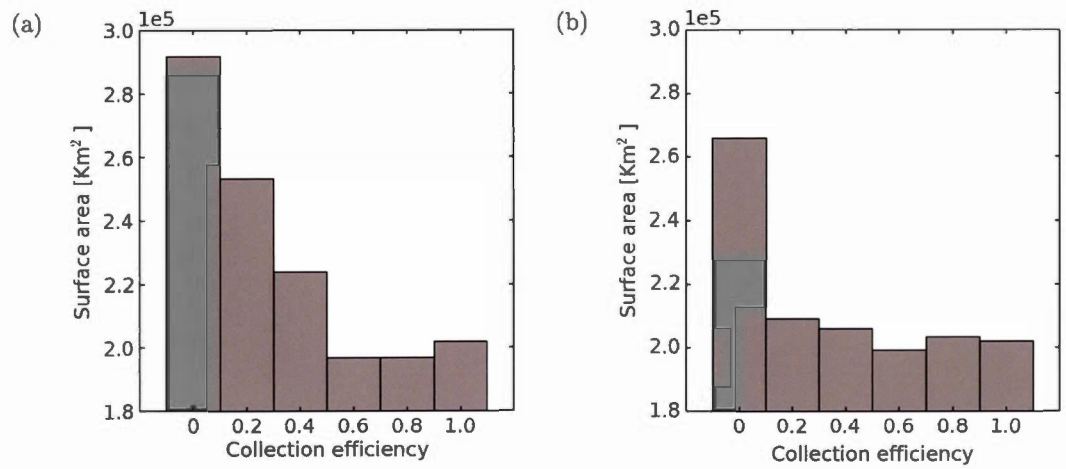

Figure 2.18: Surface area (km^2) with an accumulation of freezing rain in excess of 0.1 mm integrated over the domain from 0000 UTC 24 December 2014 to 1800 UTC 24 December 2014. (a) E_{rg} is systematically varied while E_{ri}, $E_{rs} = 1$ (b) E_{ri} and E_{rs} are systematically varied while $E_{rg} = 1$.

CHAPITRE III

CONCLUSION

Le but de cette étude était d'examiner l'impact du gel par collision sur les précipitations en surface dans un modèle en trois dimensions. Nous avons identifié une tempête de pluie verglaçante pour laquelle le modèle HRDPS d'Environnement et Changement climatique Canada (ECCC) couplé avec le schéma microphysique MY2 a bien prédit les quantités totales de précipitation, mais a sous prévu les quantités de pluie verglaçante. Nous avons montré que ce résultat est principalement causé par le paramétrage des processus de gel par collision. En effet, le schéma MY2 a prévu correctement les quantités de précipitation totales, par contre, le schéma diagnostique de types de précipitation de Bourgouin (2000) a fait un meilleur diagnostique de leur type. Le problème n'est donc pas relié au profil vertical de température prédit par le modèle, mais plutôt au paramétrage des processus microphysiques produisant de la pluie verglaçante.

Afin de montrer l'impact du gel par collision sur la production de pluie verglaçante, plusieurs tests de sensibilité ont été menés. Premièrement, nous avons introduit une température seuil de regel pour le gel par collision. Nous l'avons fait varier systématiquement pour étudier son influence sur les quantités de pluie verglaçante prévues. Nous avons ainsi montré que ce paramètre modifie significativement les

quantités de pluie verglaçante prévues. Pour cette tempête, il est responsable du regel de plus de 90% de la pluie verglaçante. Nous avons aussi montré que la présence d'une petite quantité de glace est suffisante pour transformer une grande quantité de pluie verglaçante en glace. Également, le gel par collision a un impact plus grand sur les quantités de pluie verglaçante en surface lorsque la température de l'air est relativement chaude. Par exemple, abaisser la température de regel de 0°C à -1°C provoque un changement important sur les quantités de pluie verglaçante, tandis que l'abaisser de -4°C a -5°C a un effet négligeable. Ceci est attribuable au fait que de plus grandes quantités d'eau surfondue se retrouvent dans l'atmosphère lorsque la température de l'air se rapproche du point de congélation. Finalement, puisqu'on retrouve des quantités importantes d'eau surfondue sous une couche de fonte en altitude, la température seuil de regel affecte principalement les types de précipitation prévus à cet endroit.

Deuxièmement, l'impact du paramètre d'efficacité de collecte entre les particules solides et liquides a été examiné en le faisant varier de façon systématique. Ceci a été fait en deux temps. Une première série d'expériences dans lesquelles l'efficacité de collecte pour les termes de collisions pluie-glace et la pluie-neige a été variée tout en gardant l'efficacité pluie-graupel constante a été réalisée. Ces deux termes n'ont pas besoin de la présence de graupel pour être actifs ; ce sont plutôt des termes qui génèrent du graupel. Dans une deuxième série d'expériences, l'efficacité de collecte pour le terme pluie-graupel a été systématiquement modifiée tout en gardant les termes de collisions pluie-glace et pluie-neige constants. Contrairement aux autres termes, le terme de collision de pluie-graupel requiert la présence de graupel pour être actif. Il a été démontré que ce terme a un impact important sur les quantités prévues de pluie verglaçante, tandis que les deux premiers n'ont qu'un effet négligeable.

Les résultats montrent que le gel par collision est un processus rapide. Ceci

pourrait être expliqué par le fait que dans les schémas de type bulk, la température des particule est présumée égale à celle de l'air. Dans la nature, les gouttes de pluie qui se forment dans la couche de fonte puis tombent dans un environnement avec de l'air plus froid sont plus chaudes que leur environnement, et ce, jusqu'à ce que leur chaleur se dissipe dans l'environnement. Quant à elles, les particules en phase mixte ont une température de 0°C. Lorsqu'elles se trouvent dans la couche de regel, elles sont donc nécessairement plus chaudes que leur environnement. Pour ces deux raisons, il probable que dans les schémas de type bulk la température des gouttes d'eau dans la couche de regel est sous-estimée, causant un regel beaucoup plus rapide des particules que ce qui se produit dans la nature.

Le gel par collision est paramétré dans les schémas bulk comme un processus complet et instantané. Dans la nature, il s'agit plutôt d'un processus rapide, mais non instantané (Rogers and Yau, 1989; Pruppacher and Klett, 1997; Hindmarsh *et al.*, 2003). Dans la nature, juste au dessus de la couche chaude, lorsque la température avoisine 0°C, le gel par collision peut mener à la formation d'hydrométéores en phase mixte qui tombent ensuite dans la couche chaude. Ceux-ci fondent plus rapidement que s'ils étaient complètement glacées car ils contiennent moins de glace. On peut donc supposer que dans la nature, les particules formées au dessus de la couche de fonte vont fondre plus rapidement dans la couche de fonte, que ce qui est représenté dans un schéma bulk. Dans un schéma bulk, la quantité de particules solides qui traversent la couche chaude sans fondre, et qui sont disponibles pour initier le gel par collision dans la couche froide pourrait donc être surestimée.

L'absence de la représentation des particules en phase mixte augmente les chances de collisions entre les particules. Dans le paramétrage de la fonte des particules, l'eau est instantanément séparée de la glace. La particule qui est en phase mixte

dans la nature est donc représentée par deux particules distinctes dans les schémas bulk. Ces deux particules de taille et densité différentes ont des vitesses terminales de chute différentes. Elles peuvent donc entrer en collision. Dans la nature, puisque la particule reste entière lors de la fonte, le gel par collision n'accélère pas son regel. C'est pour cette raison que l'absence de particules en phase mixte peut augmenter le taux de gel par collision dans les schémas bulk. Dans les schémas bulk, la fonte serait mieux représentée si la phase mixte était paramétrée.

Le schéma MY2 conserve la masse moyenne de la particule la plus volumineuse plutôt que le nombre de particules lors du gel par collision. Comme les interactions entre les particules liquides et solides sont complexes dans la nature, ceci est simplement un choix de paramétrage qui a été fait. Dans la nature, les particules glacées n'ont pas une densité constante. Les particules solides, telles que les flocons, sont remplies d'interstices d'air. Lors d'une collision entre une particule solide et une particule liquide, certains de ces interstices peuvent se remplir d'eau. La façon de paramétrer le nombre de particules résultantes d'une collision et par conséquent, leur volume et diamètre, est très délicate. Puisque le nombre de particules de chaque catégorie est directement utilisé dans les calculs de gel par collision, il serait souhaitable d'explorer l'impact d'une variation de ce paramétrage sur le gel par collision et sur les quantités de pluie verglaçantes prévues en surface.

En l'absence d'une catégorie de particules semi-liquides dans le schéma MY2, une température seuil pour le gel par collision de $-5°C$ devrait être introduite afin de limiter la collecte excessive de la pluie verglaçante par le graupel. Lorsque la température est près du point de congélation, le paramétrage de la température des particules est extrêmement difficile. Une façon de pallier cette difficulté serait de limiter le gel par collision lorsque les températures sont relativement chaudes. Une seconde avenue serait de réduire l'efficacité de collecte entre les particules de

pluie et de graupel. Par contre, pour la tempête que nous avons étudiée, il serait nécessaire de définir l'efficacité de collecte entre la pluie et le graupel comme étant nulle, pour que les quantités de pluie verglaçante se rapprochent des observations.

Les conclusions de cette étude sont spécifiques à cette tempête. Ce problème a cependant été noté pendant plusieurs autres tempêtes durant l'hiver 2014-2015. Des différences de l'ordre de 5 à 10 mm entre les quantités de pluie verglaçante prévues par le Système Régional de Prévision Déterministe (SRPD) et le Système à Haute Résolution de Prévision Déterministe (SHRPD) ont été notées. La prévision du SRPD étant plus près des observations, une température seuil de regel de $-5°C$ pour le gel par collision a été introduite dans la version opérationnelle du SHRPD le 15 décembre 2015. Ceci a amélioré la prévision de quantité de pluie verglaçante par ce modèle. Nous pensons donc que les conclusions de ce travail pourraient être généralisées à d'autres tempêtes.

Les travaux futurs pourraient porter sur l'inclusion de particules semi-liquides dans les schémas bulk et leurs effets sur le gel par collision et sur les quantités de pluie verglaçantes prévues. Ce type d'étude a déjà été réalisé en 1 dimension (Thériault and Stewart, 2010). Il a alors été démontré que l'implémentation des particules en phase mixte avait un effet notable sur les types de précipitation en surface. Ces études devraient être refaites avec un modèle atmosphérique complet. Il serait aussi intéressant d'explorer les impacts de la représentation de la vitesse terminale de chute de la neige, de sa densité, du choix des paramètres de la fonction gamma, ou du choix de conserver la masse moyenne de la particule la plus volumineuse plutôt que le nombre de particules lors du gel par collision.

ANNEXE A

THE COLLECTION EQUATION

During a unit time, a collector particle of radius R sweeps out a number of droplets $(n(r))$ of radius r, with an collection efficiency of $E(R,r)$ on its path. The total rate of increase in volume (V) of the collector drop is thus given by equation :

$$\frac{dV}{dt} = \int_0^\infty [\pi(R+r)^2[u(R)-u(r)]n(r)\frac{4\pi r^3}{3}E(R,r)dr \qquad (A.1)$$

$u(r), u(R)$ are the terminal fall velocities of the collector and collected particles. The total increase in number (N) and mixing ratio (Q) of the spectrum of collector drops in a unit space is then calculated using the following equations :

$$\frac{dQ}{dt} = \int_0^\infty \int_0^\infty \pi(R+r)^2[u(R)-u(r)]m(r)n(r)n(R)E(R,r)drdR \qquad (A.2)$$

$$\frac{dN}{dt} = \int_0^\infty \int_0^\infty \pi(R+r)^2[u(R)-u(r)]n(r)n(R)E(R,r)drdR \qquad (A.3)$$

Where m and n represent the mass and number concentration of particles.

ANNEXE B

MODEL COMPARISON

For the purpose of reducing the numerical costs of this study, all the sensitivity tests were performed on a subdomain of the operational HRDPS domain. We consider that the main storm features for the event of 24-25 December 2014 were reproduced on this subdomain. After 36 h of integration, the sea level pressure features from both runs were similar : the low pressure centers and troughs are collocated and have similar surface pressures. The instantaneous precipitation field is very sensitive to small changes in the dynamics and thermodynamics of the storm and therefore it can be used to verify that both model runs were equivalent. After 36 h of integration, the location, intensity and structure of the instant precipitation rates are similar. Finally, a comparison of the total freezing rain amounts forecast after 36 h of integration showed both runs were very comparable. It is then acceptable to conclude that the HRDPS and CTR are equivalent.

RÉFÉRENCES

Bergeron, T. (1935). On the physics of clouds and precipitation. *Procès Verbaux de l'Association de Météorologie*, pages 156—178.

Bigg, E. K. (1953). The supercooling of water. *Proceedings of the Physical Society. Section B*, 66(8), 688.

Bourgouin, P. (2000). A method to determine precipitation types. *Weather and Forecasting*, 15(5), 583–592.

Brandes, E. A., Ikeda, K., Zhang, G., Schönhuber, M., and Rasmussen, R. M. (2007). A statistical and physical description of hydrometeor distributions in colorado snowstorms using a video disdrometer. *Journal of Applied Meteorology and Climatology*, 46(5), 634–650.

Carmichael, H., Stewart, R., Henson, W., and Thériault, J. (2011). Environmental conditions favoring ice pellet aggregation. *Atmospheric Research*, 101(4), 844–851.

Caron, J.-F., Milewski, T., Buehner, M., Fillion, L., Reszka, M., Macpherson, S., and St-James, J. (2015). Implementation of deterministic weather forecasting systems based on ensemble-variational data assimilation at Environment Canada. Part ii: The regional system. *Monthly Weather Review*, 143(7), 2560–2580.

Cober, S. G. and List, R. (1993). Measurements of the heat and mass transfer parameters characterizing conical graupel growth. *Journal of the Atmospheric Sciences*, 50(11), 1591–1609.

Cohard, J.-M. and Pinty, J.-P. (2000). A comprehensive two-moment warm microphysical bulk scheme. i: Description and tests. *Quarterly Journal of the Royal Meteorological Society*, 126(566), 1815–1842.

Cooper, W. A. (1986). Ice initiation in natural clouds. In *Precipitation Enhancement A Scientific Challenge*, pages 29–32. Springer.

Cortinas, J. V., Bernstein, B. C., Robbins, C. C., and Walter Strapp, J. (2004). An analysis of freezing rain, freezing drizzle, and ice pellets across the United States and Canada: 1976-90. *Weather and Forecasting*, 19(2), 377–390.

Ferrier, B. (1994). A double-moment multiple-phase four-class bulk ice scheme. Part I: Description. *Journal of the Atmospheric Sciences*, 51(2), 249–280.

Fletcher, N. (1958). Size effect in heterogeneous nucleation. *The Journal of Chemical Physics*, 29(3), 572–576.

Fletcher, N. (1969). Active sites and ice crystal nucleation. *Journal of the Atmospheric Sciences*, 26(6), 1266–1271.

Geresdi, I. (1998). Idealized simulation of the colorado hailstorm case: Comparison of bulk and detailed microphysics. *Atmospheric Research*, 45(4), 237–252.

Gibson, S. R. and Stewart, R. E. (2007). Observations of ice pellets during a winter storm. *Atmospheric Research*, 85(1), 64–76.

Hallett, J. (1974). Production of secondary ice particles during the riming process. *Nature*, 249, 26–28.

Hanesiak, J. M. and Stewart, R. E. (1995). The mesoscale and microscale structure of a severe ice pellet storm. *Monthly Weather Review*, 123(11), 3144–3162.

Hindmarsh, J., Russell, A., and Chen, X. (2003). Experimental and numerical analysis of the temperature transition of a suspended freezing water droplet. *International Journal of Heat and Mass Transfer*, 46(7), 1199–1213.

Hong, S.-Y. and Lim, J.-O. J. (2006). The wrf single-moment 6-class microphysics scheme (wsm6). *Journal of Korean Meteorological Society*, 42(2), 129–151.

Kain, J. S. and Fritsch, J. M. (1993). Convective parameterization for mesoscale models: The Kain-Fritsch scheme. In *The representation of cumulus convection in numerical models*, pages 165–170. Springer.

Khain, A., Pinsky, M., Shapiro, M., and Pokrovsky, A. (2001). Collision rate of small graupel and water drops. *Journal of the Atmospheric Sciences*, 58(17), 2571–2595.

Langham, E. and Mason, B. (1958). The heterogeneous and homogeneous nucleation of supercooled water. *Proceedings of the Royal Society of London A: Mathematical, Physical and Engineering Sciences*, 247(1251), 493–504.

Li, J. and Barker, H. (2005). A radiation algorithm with correlated-k distribution. Part i: Local thermal equilibrium. *Journal of the Atmospheric Sciences*, 62(2), 286–309.

Mailhot, J. and Bélair, S. (2002). An examination of a unified cloudiness-turbulence scheme with various types of cloudy boundary layers. *Preprints, 15th Symposium on Boundary Layer and Turbulence, Wageningen, Netherlands, American Meteorological Society*, 15, 215–218.

Mailhot, J., Bélair, S., Lefaivre, L., Bilodeau, B., Desgagné, M., Girard, C., Glazer, A., Leduc, A.-M., Méthot, A., Patoine, A., et al. (2006). The 15-km version of the Canadian regional forecast system. *Atmosphere-Ocean*, 44(2), 133–149.

Meyers, M. P., DeMott, P. J., and Cotton, W. R. (1992). New primary ice-nucleation parameterizations in an explicit cloud model. *Journal of Applied Meteorology*, 31(7), 708–721.

Milbrandt, J. and Yau, M. (2005a). A multimoment bulk microphysics parameterization. Part I: Analysis of the role of the spectral shape parameter. *Journal of the Atmospheric Sciences*, 62(9), 3051–3064.

Milbrandt, J. and Yau, M. (2005b). A multimoment bulk microphysics parameterization. Part II: A proposed three-moment closure and scheme description. *Journal of the Atmospheric Sciences*, 62(9), 3065–3081.

Milbrandt, J. A., Bélair, S., Faucher, M., Vallée, M., Carrera, M. L., and Glazer, A. (2016). The Pan-Canadian high resolution (2.5 km) deterministic prediction system. *Weather and Forecasting*, 31(6), 1791–1816.

Mitra, S., Vohl, O., Ahr, M., and Pruppacher, H. (1990). A wind tunnel and theoretical study of the melting behavior of atmospheric ice particles. iv: Experiment and theory for snow flakes. *Journal of the Atmospheric Sciences*, 47(5), 584–591.

Noilhan, J. and Planton, S. (1989). A simple parameterization of land surface processes for meteorological models. *Monthly Weather Review*, 117(3), 536–549.

Pitter, R. and Pruppacher, H. (1974). A numerical investigation of collision efficiencies of simple ice plates colliding with supercooled water drops. *Journal of the Atmospheric Sciences*, 31(2), 551–559.

Pruppacher, H. R. and Klett, J. D. (1997). *Microphysics of Clouds and Precipitation*. Springer Science & Business Media, 954 pp., 2 edition.

Reisner, J., Rasmussen, R. M., and Bruintjes, R. (1998). Explicit forecasting of supercooled liquid water in winter storms using the MM5 mesoscale model. *Quarterly Journal of the Royal Meteorological Society*, 124(548), 1071–1107.

Rogers, R. R. and Yau, M. K. (1989). *A short course in cloud physics*. Pergamon Pres, 235 pp., 2 edition.

Saleeby, S. M. and Cotton, W. R. (2008). A binned approach to cloud-droplet riming implemented in a bulk microphysics model. *Journal of Applied Meteorology and Climatology*, 47(2), 694–703.

Stewart, R. and Crawford, R. (1995). Some characteristics of the precipitation formed within winter storms over eastern newfoundland. *Atmospheric Research*, 36(1), 17–37.

Stewart, R. E. (1992). Precipitation types in the transition region of winter storms. *Bulletin of the American Meteorological Society*, 73(3), 287–296.

Stewart, R. E., Thériault, J. M., and Henson, W. (2015). On the characteristics of and processes producing winter precipitation types near 0°C. *Bulletin of the American Meteorological Society*, 96(4), 623–639.

Straka, J. M. and Mansell, E. R. (2005). A bulk microphysics parameterization with multiple ice precipitation categories. *Journal of Applied Meteorology*, 44(4), 445–466.

Sundqvist, H. (1988). Parameterization of condensation and associated clouds in models for weather prediction and general circulation simulation. In *Physically-based modelling and simulation of climate and climatic change*, pages 433–461.

Thériault, J. M. and Stewart, R. E. (2010). A parameterization of the microphysical processes forming many types of winter precipitation. *Journal of the Atmospheric Sciences*, 67(5), 1492–1508.

Thompson, G., Field, P. R., Rasmussen, R. M., and Hall, W. D. (2008). Explicit forecasts of winter precipitation using an improved bulk microphysics scheme. Part II: Implementation of a new snow parameterization. *Monthly Weather Review*, 136(12), 5095–5115.

Thompson, G., Rasmussen, R. M., and Manning, K. (2004). Explicit forecasts of winter precipitation using an improved bulk microphysics scheme. Part I: Description and sensitivity analysis. *Monthly Weather Review*, 132(2), 519–542.

Verlinde, J., Flatau, P. J., and Cotton, W. R. (1990). Analytical solutions to the collection growth equation: Comparison with approximate methods and application to cloud microphysics parameterization schemes. *Journal of the Atmospheric Sciences*, 47(24), 2871–2880.

Zerr, R. J. (1997). Freezing rain: An observational and theoretical study. *Journal of Applied Meteorology*, 36(12), 1647–1661.